



Source area evolution and thermal record of an Early Cretaceous back-arc basin along the northwesternmost Colombian Andes



S. León^{a,b,c,*}, A. Cardona^{b,d}, D. Mejía^{b,e}, G.E. Botello^{b,f}, V. Villa^{b,f}, G. Collo^g, V. Valencia^h, S. Zapataⁱ, D.S. Avellaneda-Jiménez^b

^a Departamento de Geociencias, Facultad de Ciencias, Universidad Nacional de Colombia, Bogotá, Colombia

^b Grupo de Investigación en Geología y Geofísica EGEO, Universidad Nacional de Colombia, Medellín, Colombia

^c Smithsonian Tropical Research Institute, Balboa, Ancon, Panama

^d Departamento de Procesos y Energía, Facultad de Minas, Universidad Nacional de Colombia, Colombia

^e Departamento de Materiales y Minerales, Facultad de Minas, Universidad Nacional de Colombia, Colombia

^f Departamento de Geociencias y Medioambiente, Facultad de Minas, Universidad Nacional de Colombia, Colombia

^g Consejo Nacional de Investigaciones Científicas y Tecnológicas (CONICET), Centro de Investigaciones en Ciencias de La Tierra (CICTERRA), Argentina

^h School of the Environment, Washington State University, USA

ⁱ Institute of Earth and Environmental Sciences, University of Potsdam, Germany

ARTICLE INFO

Keywords:

Back-arc basin
Northern Andes
Early cretaceous
Provenance
Clay mineralogy
Rutile mineral chemistry

ABSTRACT

Identifying the provenance signature and geodynamic setting on which sedimentary basins at convergent margins grow is challenging since they result from coupled erosional and tectonic processes, which shape the evolution of source areas and the stress regime. The Early Cretaceous evolution of the northern Andes of Colombia is characterized by extensional tectonics and the subsequent formation of a marginal basin. The Abejorral Formation and coeval volcano-sedimentary rocks are exposed along the western flank and axis of the Central Cordillera. They comprise an Early Cretaceous transgressive sequence initially accumulated in fluvial deltaic environments, which switched towards a deep-marine setting, and are interpreted as the infilling record of a marginal back-arc basin. Available provenance data suggest that Permian-Triassic metamorphic and less abundant Jurassic magmatic rocks forming the basement of the Central Cordillera sourced the Abejorral Formation. New detailed volcanic and metamorphic lithics analyses, conventional and varietal study of heavy minerals, detrital rutile mineral chemistry, allowed us to document changes in the source areas defined by the progressive appearance of both higher-grade and more distal low-grade metamorphic sources, which switched from pelitic to dominantly mafic in composition. Crystallochemical indexes of clay minerals of fine-grained rocks of the Abejorral Formation suggest that samples located close to the Romeral Fault System show characteristics of low-medium P-T low-grade metamorphism, whereas rocks located farther to the northeast preserve primary diagenetic features, which suggest a high heat-flow accumulation setting. We interpret that the Abejorral Formation records the progressive unroofing of the Central Cordillera basement that was being rapidly exhumed, as well as the incorporation of distal subduction-related metamorphic complexes to the west in response either to the widening of extensional front or the reactivation of fault structures on the oceanward margin of the basin. Although the deformational record of the Abejorral Formation would have resulted from over-imposed episodes, our new geochronological constraints suggest that this sedimentary sequence must have been deformed before the Paleocene due to the presence of arc-related intrusive non-deformed magmatic rocks with a crystallization age of ca. 60 Ma.

1. Introduction

Provenance analyses are widely used in order to unravel the geodynamic setting on which sedimentary basins were formed, as well as the tectonic mechanisms responsible for their growth and evolution

(Garzanti et al., 2007; Morton and Hallsworth, 1999; von Eynatten and Dunkl, 2012; Weltje and von Eynatten, 2004). Yet, the reconstruction of mechanisms responsible for the evolution of sedimentary basins at convergent margins, such as back-arc basins, is not always straightforward since they result from complex interactions between tectonics

* Corresponding author. Departamento de Geociencias, Facultad de Ciencias, Universidad Nacional de Colombia, Colombia.
E-mail address: saleonv@unal.edu.co (S. León).

<https://doi.org/10.1016/j.jsames.2019.102229>

Received 20 March 2019; Received in revised form 10 June 2019; Accepted 10 June 2019

Available online 11 June 2019

0895-9811/ © 2019 Elsevier Ltd. All rights reserved.

and erosion/sedimentation processes including the mode and rates of subsidence, basin geometry, as well as the location and magnitude of exhumation/erosion (e.g. [Burov and Poliakov, 2003](#)). Moreover, the subsequent occurrence of multiple deformational episodes during the protracted tectonic evolution of back-arc basins result in complex structural overprinting of associated rocks, which may obscure the textural and mineralogical features imprinted by the stress and thermal regime on which the basin was initially formed (e.g. [Klepeis et al., 2010](#); [Munteanu et al., 2011](#)).

Hence, the spatial and temporal evolution of the source areas and the basin itself, triggered by modifications of the subduction system (i.e. dip-angle, obliquity, upper-plate thermal state), led to complex provenance and deformational features, which need to be addressed from a multi-technical approach including detailed petrographic, geochemical and mineralogical analyses (e.g. [Reimann-Zumsprekel et al., 2015](#); [Schneider et al., 2017](#)). In orogenic belts with complex metamorphic, plutonic and sedimentary associations, conventional provenance analysis may result in ambiguous identification of source areas, which may share common lithological and compositional, or even geochronological signatures (e.g. [von Eynatten and Dunkl, 2012](#)). Furthermore, jointly studying the mineralogy and crystallochemical changes of clays as response to the P-T conditions of diagenesis and/or low-grade metamorphism (e.g. [Verdecchia et al., 2018](#)), allow assessing the pressure-temperature conditions on which sedimentary basins grew and were subsequently deformed ([Stone and Merriman, 2004](#)). However, this is hard to be solved solely from stratigraphic and provenance analyses (e.g. [Corrado et al., 2018](#)).

The Early Cretaceous evolution of the northern Colombian Andes was shaped by a period of tectonic extension and generation of marginal basins, which can be traced along the entire Andean margin (e.g. [Atherton and Webb, 1989](#); [Braz et al., 2018](#); [Stern and De Wit, 2003](#); [Zapata et al., 2019](#)). The stratigraphic record of such geodynamic setting is well preserved in Lower Cretaceous siliciclastic marine-deltaic sequences exposed in the Magdalena Valley and the Eastern Cordillera of Colombia ([Duarte et al., 2018](#); [Sarmiento-Rojas et al., 2006](#)), and coeval isolated sedimentary rocks exposed along both flanks and the axis of the Central Cordillera of Colombia ([González, 2001](#); [Maya and González, 1995](#), [Fig. 1](#)). These Lower Cretaceous rocks unconformably overlie the pre-Cretaceous metamorphic basement of the Central Cordillera, and are characterized by a transgressive nature. Moreover, they are commonly associated with basaltic-andesitic lava units and occasionally with fragmented ophiolite remnants ([Álvarez, 1987](#); [Arévalo et al., 2001](#); [Gómez-Cruz et al., 1995](#); [González, 2001](#); [Nivia et al., 2006](#); [Zapata et al., 2019](#)).

In this contribution, we present the results of a high-resolution provenance analysis including detailed sandstone petrography (i.e. textural discrimination of metamorphic and volcanic lithic fragments), heavy minerals and rutile mineral chemistry, as well as clays crystallochemical indexes such as the Kübler Index ([Kübler, 1968](#)) and b parameter ([Sassi and Scolari, 1974](#)) as thermobarometric constraints. A complementary geochronological analysis of an arc-related unit intruding the Lower Cretaceous rocks was conducted in order to provide a maximum age for the occurrence of a major deformational episode in the studied sedimentary sequence. Our multi-technical approach attempts to address the link between erosional/exhumation patterns of source areas, the stratigraphy and the thermal signature of a marginal basin in response to extensional tectonics.

2. Geological context

The evolution of the northern Colombian Andes during the Early Cretaceous was shaped by a period of extensional tectonics ([Braz et al., 2018](#); [Sarmiento-Rojas et al., 2006](#); [Villamil and Pindell, 1999](#)). Diachronous marine-deltaic siliciclastic sequences accumulated over the pre-Cretaceous continental basement and are exposed along the Eastern and Central Cordilleras, as well as in the Magdalena Valley ([Duarte](#)

[et al., 2015](#); [Sarmiento-Rojas et al., 2006](#); [Villamil and Pindell, 1999](#), [Fig. 1](#)).

Lower Cretaceous sedimentary rocks of the Central Cordillera are included within several units, such as Valle Alto, San Pablo, La Soledad and Abejorral Fms., San Luis, Segovia, Amalfi, and Berlin Sediments, as well as the Quebradagrande Complex ([Arévalo et al., 2001](#); [Gómez-Cruz, 1995](#); [González, 2001, 1980](#); [Quiroz, 2005](#); [Rodríguez and Rojas, 1985](#); [Villagómez et al., 2011](#)). These units are commonly defined by basal quartz-rich coarse-grained deposits interpreted as accumulated on fluvial-deltaic settings, which are gradually replaced by fine-grained marine rocks often associated with the occurrence of basaltic-andesitic lava, gabbros and serpentinized peridotites, remnants of a fragmented ophiolite ([Arévalo et al., 2001](#); [González, 1980](#); [Nivia et al., 2006](#); [Zapata et al., 2019](#)).

The Quebradagrande Complex and the Abejorral Formation are the westernmost Lower Cretaceous volcano-sedimentary units exposed on the Central Cordillera, where the former is tectonically juxtaposed with middle-to high-pressure metabasic and metapelitic rocks of the contemporaneous Arquía Complex ([Avellaneda-Jiménez et al., 2019](#), and references therein; [Fig. 1](#)). Both the westernmost rocks of the Lower Cretaceous sedimentary units and the metamorphic rocks of the Arquía Complex are spatially related to the influence area of the Romeral Fault System (RFS, e.g. [Vinasco and Cordani, 2012](#)). This fault system has been interpreted as the easternmost suture zone between the continental paleomargin and the Cretaceous and younger accreted oceanic terranes derived from the Caribbean plate ([Restrepo and Toussaint, 1988](#)).

The Abejorral Formation is characterized by basal texturally immature quartzose coarse-grained conglomerates and sandstones, which unconformably overly and are in fault contact with pre-Cretaceous metamorphic rocks of the Central Cordillera basement (e.g. Cajamarca Complex). These rocks are interpreted as the record of fluvial-deltaic sedimentation and have been informally included within the lower member of the Abejorral Formation. Conversely, the informal upper member of this formation includes fine-grained carbonaceous mudstones and minor muddy sandstones of marine affinity, occasionally interlayered with basic-intermediate volcanic rocks ([Zapata et al., 2019](#)). Both members show evidences of ductile and brittle deformation as suggested by the presence of west-vergent asymmetric folding and thrust faulting with variable development of mylonitic fabrics ([González, 2001](#)).

Based on the transgressive nature, the intimate relationship with the continental basement, the occurrence of calc-alkaline magmatism to the top and the association with ophiolitic remnants linked to the formation of oceanic crust, the Early Cretaceous sedimentary record of the Central Cordillera is interpreted as the infilling of a back-arc basin ([Nivia et al., 2006](#); [Zapata et al., 2019](#)). However, previous models have also interpreted these sequences as accumulated in alternative settings such as passive margins or foreland basins (e.g. [Pardo-Trujillo et al., 2002](#); [Spikings et al., 2015](#)).

These Lower Cretaceous sedimentary rocks have been interpreted as the stratigraphic record of a passive margin setting due to the apparent absence of coeval volcanism, since spatially and temporally related volcanic units of the northern Central Cordillera are associated with an allochthonous origin ([Pardo-Trujillo et al., 2002](#); [Rodríguez and Celada-Arango, 2018](#); [Toussaint and Restrepo, 1996](#)). Alternatively, [Villagómez et al. \(2011\)](#) and [Spikings et al. \(2015\)](#) proposed that the Abejorral Formation accumulated in a foreland basin based on: i) the apparent cessation of arc-related magmatism at ca. 115 Ma, and ii) a period of rapid cooling/exhumation of a proto-Central Cordillera during ~120-100 Ma, interpreted as evidence for the transition from extensional to compressional tectonics.

Recently published geochronological, isotopic, geochemical and petrographic constraints of Lower Cretaceous volcanic and sedimentary rocks of the western Central Cordillera, suggest that the Abejorral Formation and coeval units formed in an extensional back-arc basin

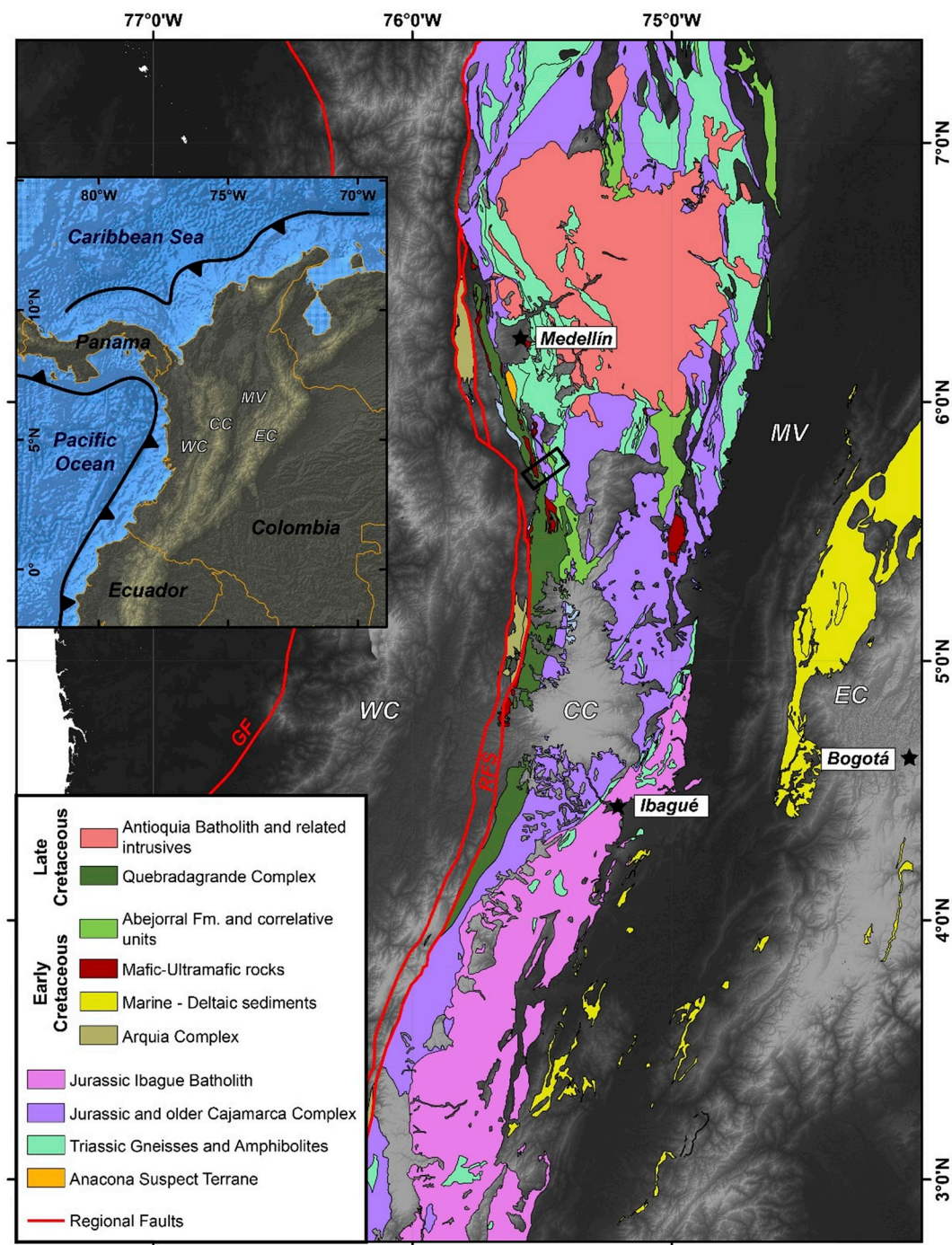


Fig. 1. Regional map showing the main lithostratigraphic domains exposed along the Central Cordillera of Colombia, the southern Magdalena Valley, and western foothills of the Eastern Cordillera. Modified from Gómez-Tapias et al. (2017). GF = Garrapatas Fault, RFS = Romeral Fault System, WC = Western Cordillera, CC = Central Cordillera, EC = Eastern Cordillera, MV = Magdalena Valley. Black rectangle delimitates the study area (Fig. 2).

(Avellaneda-Jiménez et al., 2019; Zapata et al., 2019), buttressing the previous hypothesis of Nivia et al. (2006). These authors have documented the presence of supra-subduction volcanic rocks with zircon U-Pb ages between ~ 116 and 100 Ma emplaced in a thinned crust and flanked by ca. 250 Ma continental rocks (Zapata et al., 2019), whose associated sediments were sourced by both the pre-Mesozoic continental basement and a Cretaceous subduction/accretion complex located to the west (i.e. Arquia Complex). Furthermore, ca. 83 Ma U-Pb ages and Late Cretaceous fossils of volcano-sedimentary rocks of the Quebradagrande Complex (Botero, 1963; Cochrane, 2013; Pardo-Trujillo et al., 2002; Zapata et al., 2019), suggest that the accumulation

history of this unit may extend longer than previously thought and is likely part of the back-arc basin evolution (Avellaneda-Jiménez et al., 2019; Zapata et al., 2019).

Despite it has been previously suggested that the pre-Cretaceous rocks forming the basement of the Central Cordillera (i.e. Cajamarca Complex) sourced the Abejorral Formation and coeval units (Zapata et al., 2019), the erosional/exhumation history of such domain, as well as testing whether other geological units also played a role as source areas remain unexplored.

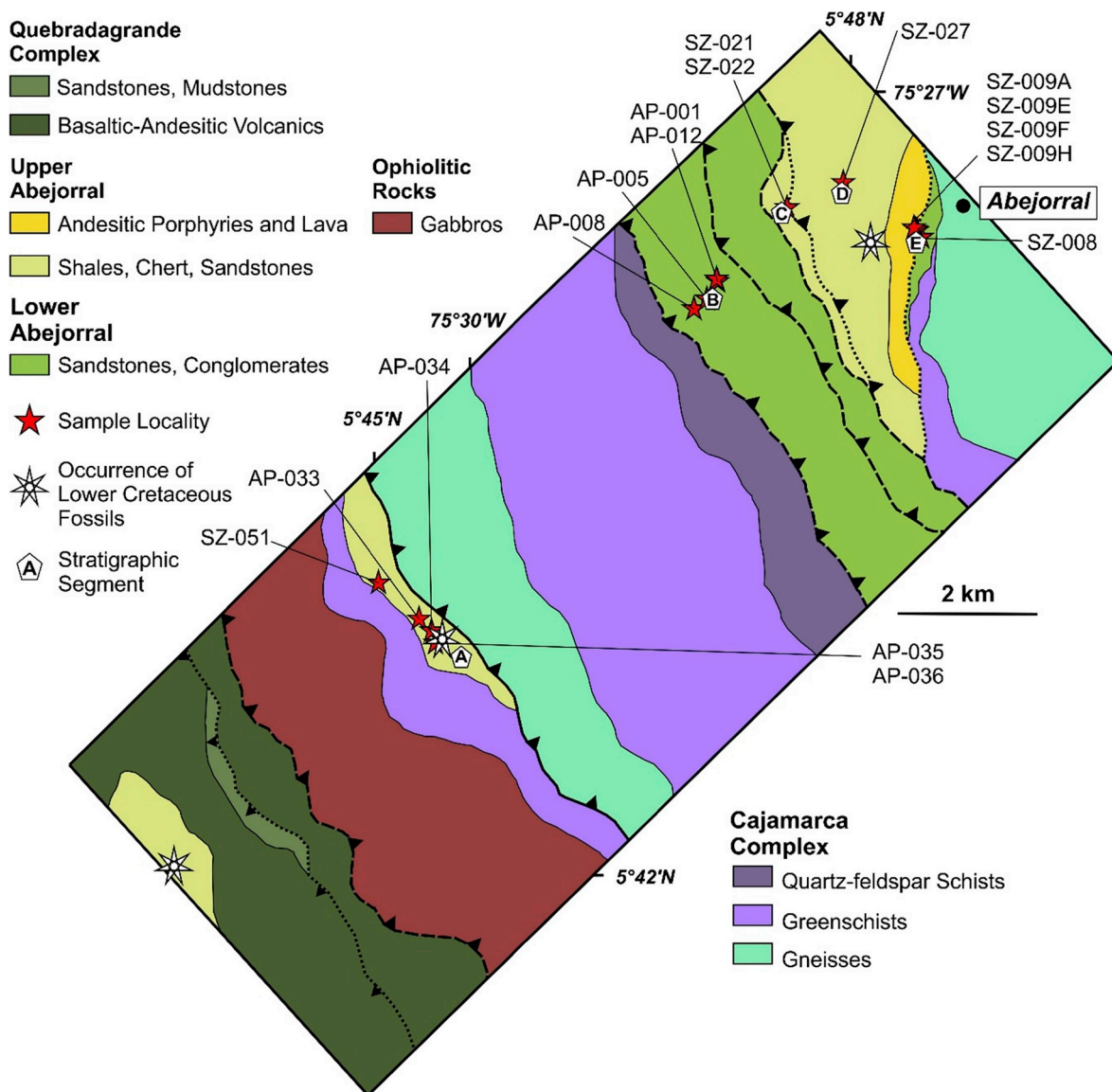


Fig. 2. Local geological map showing the main lithological units, measured stratigraphic segments and sample localities. Modified from Zapata et al. (2019).

2.1. Source areas

The axis and eastern flank of the Central Cordillera of Colombia comprise low-to high-grade Jurassic and older metamorphic rocks, locally associated with micaceous granitoids and metagabroic bodies (Blanco-Quintero et al., 2014; Bustamante et al., 2017a; Cochrane et al., 2014a; Villagómez et al., 2011; Vinasco et al., 2006; Zapata et al., 2019). These units, have been grouped within the Anaconda suspect terrane (Martens et al., 2014, Fig. 1) and the Cajamarca Complex (Maya and González, 1995), and they are intruded by intermediate-felsic Jurassic, Cretaceous and Eocene arc-related rocks (Bustamante et al., 2017b, 2016; Cardona et al., 2018; Villagómez et al., 2011; Zapata et al., 2016). The western flank of medium-to high-pressure Cretaceous metamorphic rocks, dominantly metamafic in composition with minor metapelites, grouped within the Arquía Complex, which separates parautochthonous South-American terranes from the Cretaceous and younger oceanic accreted units to the west. In this section, we present a summary of the main lithological, compositional, thermobarometric and geochronological constraints available in literature of potential source areas for the Abejorral Formation (Table 1).

3. Methodology

We have included representative sandstone samples from both the lower and upper members of the Abejorral Formation in a ca. 80 km² area in the central-northern Central Cordillera of Colombia, in proximities of the town of Abejorral (Fig. 2). Our sampling and descriptions follow the informal stratigraphic nomenclature of Zapata et al. (2019), and include some of the samples formerly described in their work. The absence of continuous exposures and the structural complexity of the region hindered the realization of a detailed stratigraphic analysis. However, we present five new stratigraphic segments in order to illustrate the main lithological features of the Abejorral Formation and provide a simplified stratigraphic framework for the analyzed samples (Fig. 3). Our simplified stratigraphic analysis, together with the revision of previously published data (Gómez-Cruz et al., 1995; González, 1980; Quiroz, 2005; Rodríguez and Rojas, 1985; Zapata et al., 2019), allowed contextualizing in a more regional framework our observations.

3.1. Volcanic and metamorphic lithics analysis

A varietal study of both metamorphic and volcanic lithic fragments, regarding their grade and composition, respectively, was conducted on

Table 1
Summary of the main lithological, mineralogical, chronological and thermobarometric features of the potential source areas for the Early Cretaceous Abejorral Formation and coeval units. Minerals abbreviations from [Sivola and Schmid \(2007\)](#).

Geological Unit	Structural Position	Dominant Lithologies	Common Mineralogy	Geochronological signature	Thermobarometric Constraints	Interpretation
Cajamarca Complex and Anaconda Suspect Terrane ^a	Basin Basement (Intrabasinal)	Orthogneisses, garnet-bearing amphibolites, amphibolites, metagabbros, quartzites, micaceous and actinolite schists	Qtz, Ms, Kfs, Bt, Chl, Act, Cpx, Hbl, Pl, Czo, Ttn, Rt, Grt, St, Ky, Zrn, Tur, And, Sil	Zircon U-Pb and K/Ar maximum accumulation ages between ~150 and 500 Ma, with older recycled ages.	Metamorphic peak mainly in amphibolite facies ~6–13 kbar and ~550–650 °C	Several lithostratigraphic domains, which record the tectonic evolution of the Colombian continental margin since the Permian-Triassic agglutination/fragmentation of Pangea to Late Jurassic terrane collision
Jurassic Intrusive Rocks ^b	Eastern Sources	Tonalites, granodiorites	Qtz, Pl, Kfs, Hbl, Bt	Zircon U-Pb and K/Ar ages between ~200 and 130 Ma		Subduction-related transtensional magmatism
Arquíu Complex ^c	Western Sources	Amphibolites, micaceous and actinolite schists, blueschists, retrograde eclogites	Qtz, Pl, Chl, Ms, Gl, Lws, Omp, Czo, Zo, Hbl, Grt, Rt, Ilm, Ttn	Garnet Lu-Hf metamorphic age of ca. 129 Ma, with K/Ar and Ar/Ar cooling ages between ~127 – 70 Ma	Decompression metamorphism ~15–10 kbar and ~640–700 °C to ~9–6 kbar and ~400–670 °C	Metamorphism of either exotic accreted oceanic crust or back-arc-related units

^a Blanco-Quintero et al., (2014); A. Bustamante et al., (2013); A. Bustamante and Juliani (2011); C. Bustamante et al., (2017a,b); Cardona et al., (2010); Cochrane et al., (2014a,b); Correa (2007); Correa et al., (2005); González (2001); Martens et al., (2014); Martens et al., (2012); Maya and González (1995); Restrepo (2008); Restrepo et al., (1991); Villagómez et al., (2011); Vinasco et al., (2006); Zapata et al., (2016).

^b Bustamante et al. (2016); Rodríguez et al. (2017); Zapata et al. (2016).

^c Bustamante (2008); Bustamante et al. (2011); García-Ramírez et al. (2017); González (2001), 1997; Maya and González (1995); McCourt et al. (1984); Orrego et al. (1980); Ríos-Reyes et al. (2008); Ruiz-Jiménez et al. (2012); Valencia-Morales et al. (2013); Villagómez et al. (2011); Villagómez and Spikings (2013).

9 samples from the lower (5) and upper (4) members of the Abejorral Formation, following the methodology proposed in [Dickinson \(1970\)](#) and [Garzanti and Vezzoli \(2003\)](#). This, in order to assess potential changes in the provenance signature due to the progressive unroofing as well as incorporation of new source areas during basin growth, which have not been explored so far.

Metamorphic lithics were subdivided according to the composition of the protolith into four groups: metapelites, metapsammites/metafelsites, metacarbonates, metabasites; and for each group, five metamorphic ranges were defined according to the increasing degree of recrystallization and progressive formation of cleavage and schistosity, following the procedure of [Garzanti and Vezzoli \(2003\)](#). The volcanic lithic fragments were classified following [Dickinson \(1970\)](#) in felsitic, microlithic, lathwork and vitreous; and according to the glass color were divided into colorless, dark-brown, light brown or green, and black. These subdivisions are related to source lithology as the glass color is thought to be a function of the rock composition and the cooling rates ([Marsaglia, 1992](#); [Schmincke, 1982](#)). Results of the high-resolution lithic analysis is presented in the supplementary material ([Table S2](#)).

3.2. Heavy minerals

Nine sandstone samples (5 from the lower and 4 from the upper members of the Abejorral Formation) were crushed, sieved and hydraulically concentrated on the Wilfley table. The 63–250 µm fraction was selected to minimize the hydraulic sorting effect and large apparent discrepancies on the mounts, following [Mange and Maurer \(1992\)](#) and [Morton \(1985\)](#). Minerals with density above 2.89 gr/cm³ were obtained by using sodium polytungstate. Mounts were prepared using the Melt-mount[®] resin with a refraction index of 1.539. A minimum of 300 translucent minerals were optically identified following the ribbon method ([Mange and Maurer, 1992](#)). Additionally, the Hornblende Color Index (HCI; [Andò et al., 2013](#)) was determined as an indicator of the temperature-pressure conditions of the potential source areas. Results of the heavy minerals conventional and varietal analysis are given in the supplementary material ([Table S3](#)).

3.3. Rutile chemistry

Chemical analyses of rutile grains were conducted on one sample from the lower member and one sample from the upper member of the Abejorral Formation. Single mineral concentrates were obtained after crushing, sieving, and hydraulically concentrating in the 63–250 µm fractions. Sodium polytungstate (2.89 gr/cm³) was used to obtain a heavy mineral concentrate to finally hand-pick the rutile crystals. The mineral chemistry analysis was conducted by using a JEOL JXA8500F field emission electron microprobe at the GeoAnalytical Lab of the Washington State University. Analyses were performed with a beam current of 20.0 nA and an accelerating voltage of 15 kV. Counting time was 20 s for all elements. Microprobe analytical error ranges ± 0.01–0.21 wt% (1σ) with detection limits varying ± 0.01–0.11 wt%. The standards used for element calibrations were albite-Cr (Na), ol-fo92 (Mg, Si), anor-hk (Al, Ca), ksp-OR1 (K), rutile1 (Ti), fayalite (Fe), rhod-791 (Mn) and chrom-s (Cr). Results are presented in the supplementary material ([Table S4](#)). Rutile grains found in the analyzed samples were classified according to [Meinhold et al. \(2008\)](#) and [Meinhold \(2010\)](#). These studies proposed that (1) rutile grains with Cr < Nb and Nb > 800 ppm are derived from metapelitic rocks (e.g. mica-schists, paragneisses, felsic granulites), (2) rutile grains with Cr > Nb, and those with Cr < Nb and Nb < 800 ppm, are derived from mafic rocks (e.g. eclogites and mafic granulites). Rutile grains from amphibolites plot in both fields because the protoliths of those rocks are of either sedimentary or mafic igneous origin. We also estimated the temperature of analyzed rutile grains following the Zr-in-rutile thermometer of [Watson et al. \(2006\)](#), in order to know the metamorphic

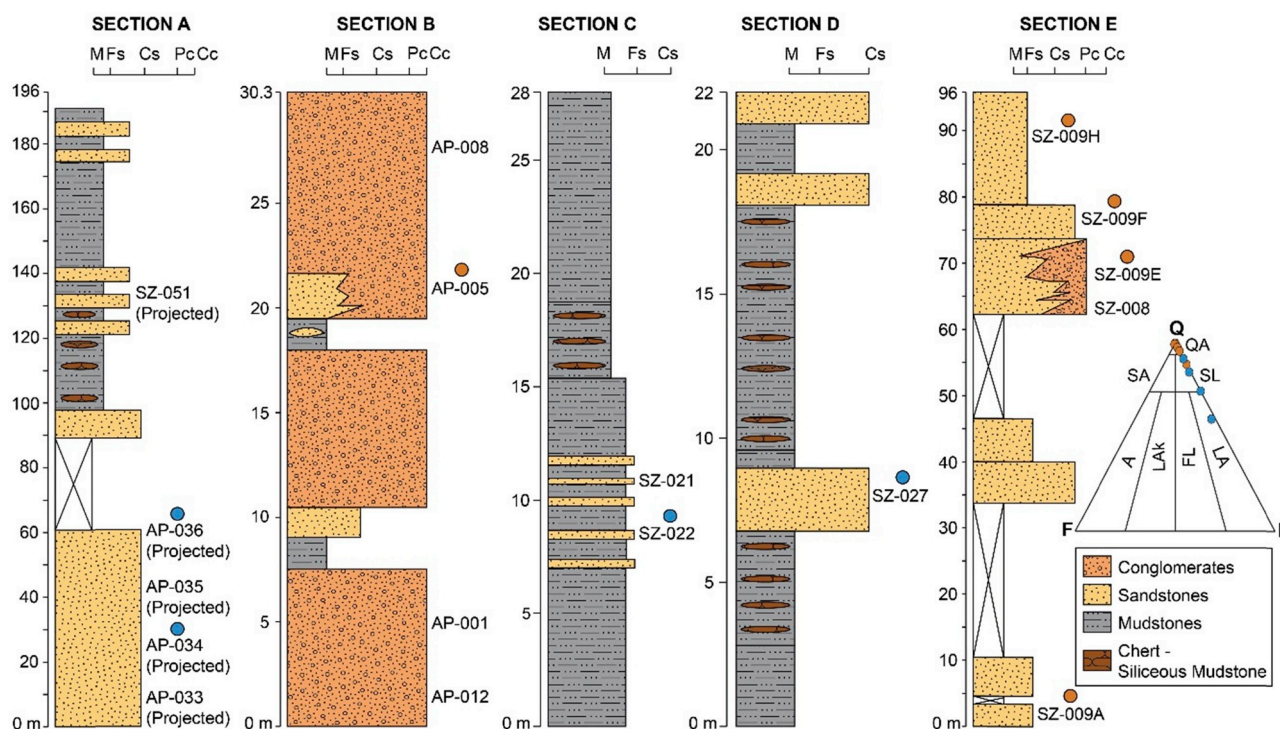


Fig. 3. Stratigraphic segments showing the main lithological associations of the Abejorral Formation within the study area and sample locations, as well as the compositional classification of sandstones, after Folk (1980). Columns B and E from the lower member, and A, C and D from the upper member. Sandstone petrographic data compiled from Zapata et al. (2019). Orange circles = lower member, blue circles = upper member. A = arkose, LAK = lithic arkose, FL = feldspathic litharenite, LA = litharenite, SA = subarkose, SL = sublitharenite, QA = quartzarenites. (For interpretation of the references to color in this figure legend, the reader is referred to the Web version of this article.)

grade of the source units for the sediments of the Abejorral Formation.

3.4. Clay minerals, Kübler Index and white mica b parameter

A total of five samples of claystones and siltstones from the Abejorral Formation were selected for the thermobarometric estimations. A petrographic analysis of each sample was carried out with the aim to recognize the diagenetic and deformational features, as well as the mineralogy, grain contacts, textures and fabric, following Kisch (1991a,b) and Weber (1981).

All XRD analyses were made and calibrated in the X PANalytical X'Pert PRO diffractometer at the Chemical Sciences Faculty of the National University of Cordoba, Argentina, and were prepared at the Clay Minerals Laboratory of the same university. The XRD analyses of the $> 2 \mu\text{m}$ fraction included two steps: first, the mineralogy was determined through XRD from the oriented clay mounts. This data was analyzed using Philips X'Pert software coupled to an International Centre for Diffraction Data (ICDD) database and the mineral phases were identified on oriented aggregates air-dried, heated at 60°C and glycolated for 12 h and heated at 500°C for 4 h. The measurements were performed with a $\text{CuK}\alpha$ radiation at 40 kV and 40 mA, $1,2^\circ/\text{min}$, between 4 and $30^\circ 2\theta$ following the recommendations of Moore and Reynolds (1997). Clay mineral phases were identified following the procedure described in Verdecchia et al. (2018). Second, the measurement of Kübler Index (KI) was determined by measuring the half-peak-width of the 10 \AA basal reflection ($\Delta^\circ 2\theta$), on the oriented clay preparations of the $< 2 \mu\text{m}$ fractions (Kübler, 1968; Warr and Rice, 1994). The KI calibration was made by measuring five polished slate standards and muscovite crystals, as proposed by Warr and Rice (1994). The KI_{CIS} (Crystallinity Index Standard, CIS) was estimated from the regression equation for the X'PertPro diffractometer: $y = 1.3885x + 0.0305 \Delta^\circ 2\theta$, $R: 0.9756$ (Warr and Rice, 1994). All the samples were prepared following the same procedure of the standards

and the values were corrected using the correlation with the CIS. Measurements were conducted with a $\text{CuK}\alpha$ radiation at 30 kV and 40 mA, $0,78^\circ/\text{min}$, between 7 and $10^\circ 2\theta$ (Kisch, 1991b; Warr and Ferreiro Mähmann, 2015; Warr and Rice, 1994).

The b parameter value of the K-white mica (\AA) is an indicator of the baric type and paleo-thermal gradients, and is based on the increase of the phengite content with increasing pressure (Ernst, 1963; Guidotti and Sassi, 1986; Kisch et al., 2006; Sassi and Scolari, 1974). The measure is carried out between $59^\circ 2\theta$ and $63^\circ 2\theta$, so that the (060) reflection of the K-white mica can be used for estimating the b value, and the (211) reflection of the quartz is used as an internal standard. Measurements conditions were 45 kV, 40 mA and $0,3^\circ/\text{min}$ with a $\text{CuK}\alpha$ radiation (Ernst, 1963; Guidotti et al., 1989; Sassi and Scolari, 1974). Results of the described mineralogical analyses are given in the supplementary material (Table S5).

3.5. Zircon U-Pb geochronology

One sample from an andesitic dyke intruding the upper member of the Abejorral Formation was selected for U-Pb geochronological analysis. Laser Ablation Inductively Coupled Plasma Mass Spectrometry (LA-ICP-MS) U-Pb analyses were conducted at Washington State University by using a New Wave Nd:YAG UV 213-nm laser coupled to a Thermo Finnigan Element 2 single collector, double-focusing, magnetic sector ICP-MS. Operating procedures and parameters were similar to those of Chang et al. (2006). The Plešovice zircon with an age of $337.13 \pm 0.37 \text{ Ma}$ (Sláma et al., 2008), was used as a standard during the analysis. Laser spot sizes and repetition rates were $30\text{--}20 \mu\text{m}$ and 10 Hz, respectively. U and Th concentrations were monitored by comparing to NIST 610 trace element glass. Zircon rims were dated to constrain the grain crystallization history (Valencia et al., 2005). Data was handled and drawn with ISOPLOT 4.15 (Ludwig, 2012), and the weighted average age is reported with a 1-sigma error. Results of the

zircon U-Pb geochronological analysis is presented in the supplementary material (Table S6).

4. Results

4.1. Geology of the study area

In the study area, a series of highly deformed micaceous quartz-feldspathic gneisses (i.e. Abejorral Gneiss, Vinasco et al., 2006), and micaceous and amphibole schists of the Cajamarca Complex (Maya and González, 1995), crop out as fault bounded NNW belts, which represent the basement of the Central Cordillera. These rocks are unconformably overlain and in fault contact with coarse-grained sediments of the Abejorral Formation, which are found in isolated exposures bounded by basement rocks (Fig. 2). To the west, gabbroic rocks from the so-called Cauca Ophiolitic Complex (Zapata et al., 2019), crop out in fault contact with volcano-sedimentary rocks of the Quebradagrande Complex. The latter, unconformably overlie a sequence of marine fine-grained rocks that are coeval with the upper member of the Abejorral Formation (Zapata et al., 2019, this work).

The Abejorral Formation includes two contrasting lithological associations, which are grouped into the lower and upper informal members, and define a dominantly transgressive sequence. The lower member (sections B and E) includes massive tabular beds of metric pebble-sized conglomerates and medium to coarse-grained sandstones, with minor gray mudstones containing sand lenses. Coarse-grained rocks have a quartz-rich composition, with sandstone samples classified as sublitharenites to quartzarenites, and conglomerates mostly composed of milky quartzose clasts (Fig. 3). The coarse-grained character of this lower member, which suggests high-energy systems, together with the common presence of plant remnants and marine fossils, allowed associating these rocks with a shoreface to fluvial-deltaic accumulation environment (Quiroz, 2005; Zapata et al., 2019, this work).

The upper member of the Abejorral Formation (sections A, C and D) consists of thick lenticular and tabular mudstone strata with subordinated fine-to medium-grained sandstones and less abundant conglomerates (González, 2001; Quiroz, 2005). Mudstone levels commonly show centimetric up to a few meters thick lenses of black chert and siliceous mudstones (Fig. 3). Sandstones from this member are more lithic-rich in composition, as well as the conglomerates, as suggested by the presence of sandstones, mudstones, intermediate volcanic and plutonic, and metamorphic rocks in clasts, with less abundant quartz (Zapata et al., 2019, Fig. 3). The mud-dominated character of the upper member of the Abejorral Formation, the dominance of marine fauna (i.e. foraminifera and bivalves), and the episodic occurrence of coarser deposits, may be interpreted as the record of sedimentation in a marine shelf or slope setting (Gómez-Cruz, 1995; Quiroz, 2005; Zapata et al., 2019, this work).

4.2. Lithic composition and heavy minerals of sandstones from the Abejorral Formation

Only one sandstone sample from the lower member of the Abejorral Formation yielded metamorphic lithic fragments (AP-005), which are solely represented by rocks with pelitic protolith, suggesting the dominance of low-grade (62%) and minor medium- (25%) to high-grade grains (13%; Fig. 4). Volcanic lithic fragments were not identified in samples from the lower member of the Abejorral Formation.

Conversely, the analyzed samples from the upper member include metamorphic lithics with both pelitic and psammitic/felsic protoliths, with the former slightly more abundant. Metapelitic lithic fragments are mostly represented by low-grade grains (up to 62.5%), but also include very low- (< 13.3%), medium- (< 10.5%) and high-grade grains (< 15.8%; Fig. 4). Lithics with psammitic/felsic protoliths include very low- (< 33.3%), low- (< 20%), medium- (< 20%), high- (< 10.5%) and very high-grade grains (< 5.3%). Volcanic lithic

fragments include colorless felsitic (< 66.7%), dark brown vitreous (< 33.3%), and green-light brown vitreous grains (up to 100%; Fig. 4). Felsitic fragments are characterized by anhedral microcrystalline mosaics, either granular or seriate, mostly composed of quartz and feldspar with a colorless glassy groundmass, which is commonly associated with silicic lavas or tuffs (Dickinson, 1970). The glass color of vitreous fragments varying from light brown to dark brown, suggests an intermediate to basic composition (Schmincke, 1982).

Heavy minerals of the lower member, mostly include stable and ultrastable species such as muscovite (~9–47%), epidote-group minerals (~3–51%), staurolite (< 7%), zircon (~13–30%), tourmaline (~3–31%) and rutile (~2–6%), with minor unstable fractions including biotite (< 5%), hornblende (~1–18%) and clinopyroxene (< 2%; Fig. 5). Identified hornblende crystals are dominantly green (~43–100%) and brown (up to ~57%), with blue-green (< 14.3%) and green-brown (< 20%). The HCI values spanning between ~33 and ~71 (Fig. 5) suggest the dominance of upper amphibolite and meta-sedimentary granulite facies rocks, or dissected arc-related batholiths of the middle-upper crust as sources (Andò et al., 2013; Garzanti and Andò, 2007).

In the analyzed samples from the upper member, heavy minerals are mostly composed of stable and ultrastable species including muscovite (~21–28%), epidote-group minerals (~8–38%), titanite (< 5%), apatite (< 1%), zircon (~19–23%), rutile (~1–12%) and tourmaline (~2–30%), with minor unstable minerals such as biotite (~1–18%) and hornblende (~1–4%; Fig. 5). The latter includes mostly the green (up to 100%), green-brown (< 50%) and brown (< 50%) varieties with blue-green species absent. HCI values ranging from ~33 to ~83 (Fig. 5), indicate that upper amphibolite, metasedimentary and meta-gabbroic granulite facies rocks, as well as dissected magmatic rocks of the middle-upper crust, were potential sources of the analyzed samples (Andò et al., 2013; Garzanti and Andò, 2007).

4.3. Rutile chemistry

Thirty-six rutile crystals from sample SZ-008 (lower member of the Abejorral Formation) were analyzed. Nb content ranges between 100 and 5129 ppm (only four grains with Nb < 800 ppm). Cr spans from 79 to 535 ppm, and Zr from 83 to 557 ppm. Rutile grains are mostly derived from metapelitic rocks (~90%) rather than from metabasic sources (~10%), as suggested in the Nb vs. Cr diagram of Meinhold et al. (2008) (Fig. 6A). The estimated temperatures for rutile grains from the lower member of the Abejorral Formation following the Zr-in-rutile thermometer of Watson et al. (2006), suggest that the metamorphic rocks that sourced these grains were in the medium-grade with temperatures between ~549 and ~696 °C (Fig. 6B).

Ten rutile grains analyzed from sample AP-033 (upper member of the Abejorral Formation), exhibit Nb, Cr and Zr contents spanning from 274 to 4016 ppm, 16–1820 ppm, and 11–3970 ppm, respectively. Rutile grains from the upper member suggest the dominance of metabasic (60%) over metapelitic (40%) sources (Fig. 6A), whereas grains from the lower member are mostly metapelitic in origin. The temperatures estimated from the Zr-in-rutile thermometer, indicate that metabasic sources span from the low-grade to the high-grade of metamorphism (~434–807 °C), and metapelitic rocks from medium-to high-grade (~612–800 °C; Fig. 6B). Estimated temperatures above 900 °C for sample AP-033 (one grain) from the upper member of the Abejorral Formation largely exceed the peak conditions for the above-described potential sources (i.e. Cajamarca and Arquía Complex). We claim that it may be related to the possible presence of zircon/baddeleyite micro-inclusions in the analyzed rutile grain, which is common for rocks with complex retrograde metamorphic paths (Degeling, 2003), such as those reported for the Arquía Complex (e.g. Ruiz-Jiménez, 2013).

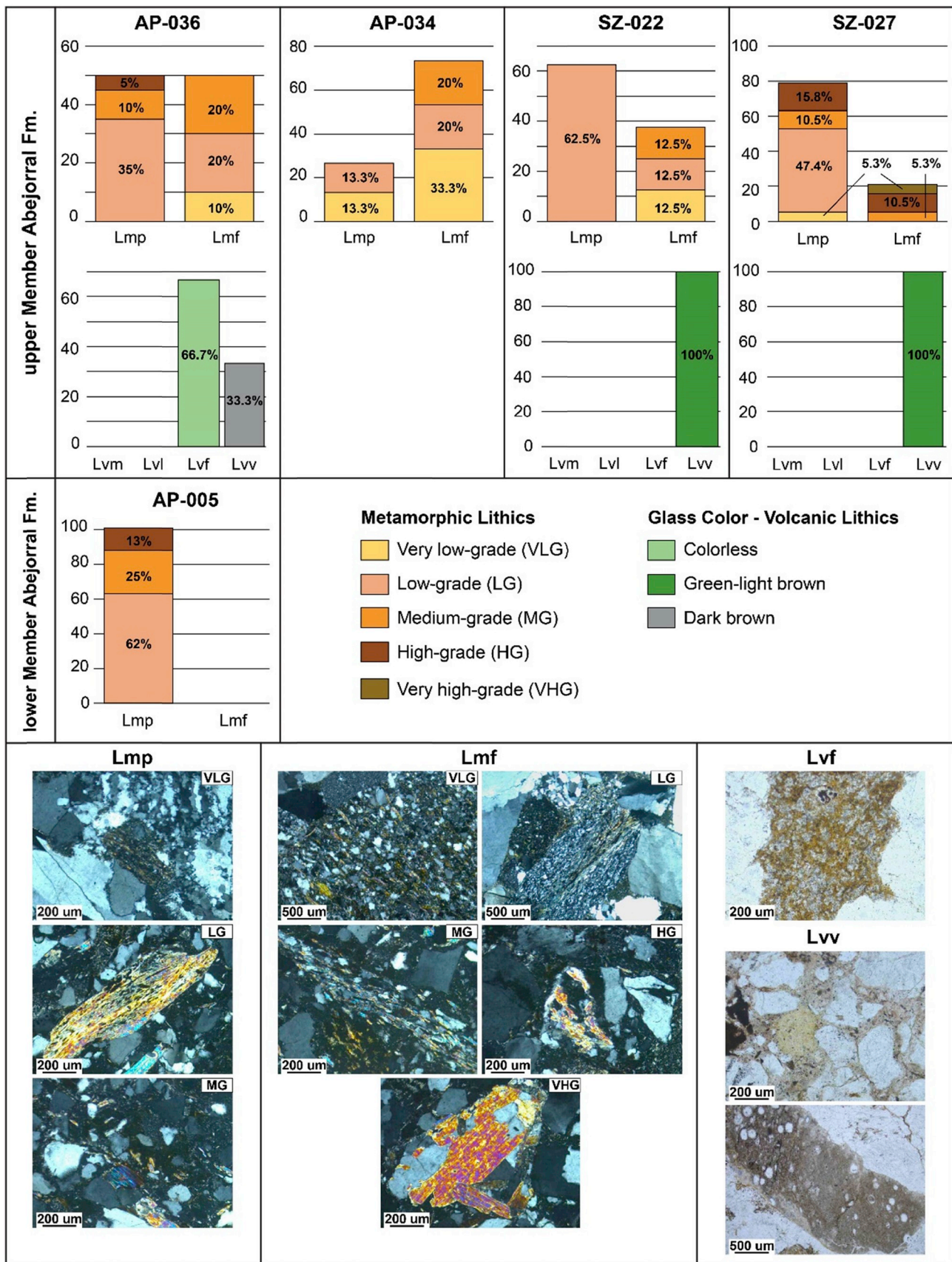


Fig. 4. Results of the lithic fragments petrographic analysis of samples from the Abejorral Formation, after Dickinson (1970) and Garzanti and Vezzoli (2003). Lmp = metapelitic, Lmf = metafelsitic, Lvm = volcanic microlithic, Lvl = volcanic lathwork, Lvf = volcanic felsitic, Lvv = volcanic vitric. For the upper member, samples are organized from west (left) to east (right).

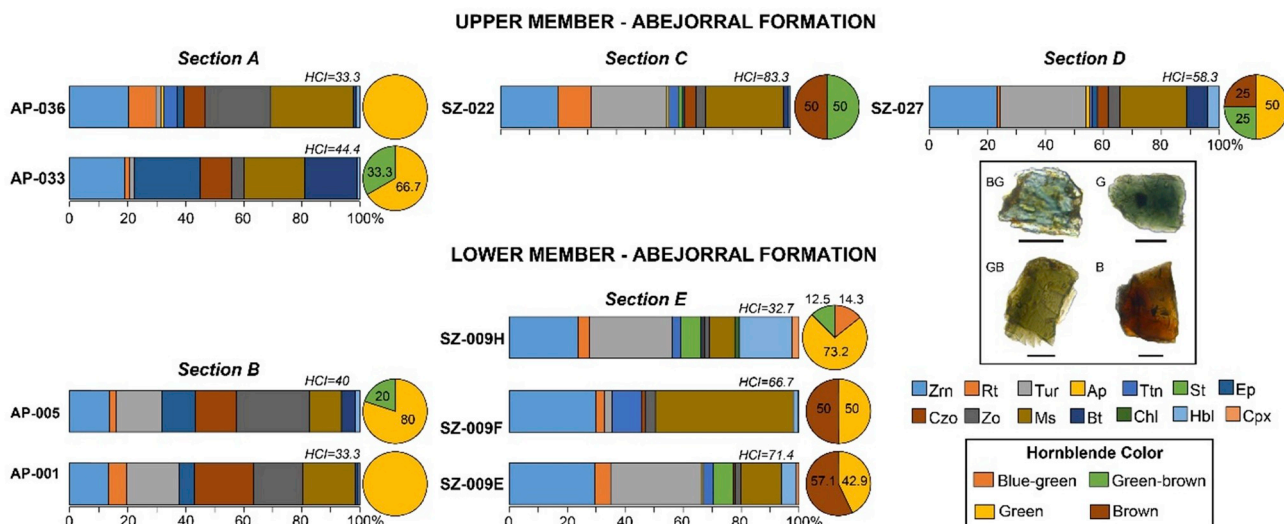


Fig. 5. Results of the heavy minerals counting (bars) and hornblende varietal analysis (pie charts) of sandstone samples from the Abejorral Formation HCI= Hornblende Color Index, after Andò et al. (2013). Within each member, samples are organized from west (left) to east (right). BG = blue-green, G = green, GB = green-brown, B = brown. (For interpretation of the references to color in this figure legend, the reader is referred to the Web version of this article.)

4.4. Clay mineralogy and crystallochemical indexes: white mica b parameter and Kübler Index

Fine-grained samples from the Abejorral Formation (lower and upper members) show contrasting sedimentary clastic and low-grade metamorphic structures, with no apparent stratigraphic control. Rocks lacking of a well-defined deformational fabric are located towards the northeast (Fig. 7A), and they are characterized by the presence of floating and punctual grain contacts, incipient spaced foliation, undulose quartz and millimetric lamination textures defined by mica and carbonaceous materials, which rarely show a poorly developed slaty cleavage. These rocks (AP-008, AP-012 and SZ-021) are mostly composed of illite, quartz, kaolinite, vermiculite, chlorite, K-feldspar?, plagioclase and gypsum? (Fig. 7B). Conversely, rocks showing a low-grade metamorphic structure (AP-035 and SZ-051) are located towards the southwest of the studied area towards the RFS (Fig. 7A), and are characterized by the presence of quartz porphyroclasts and boudins, long tangential grain contacts, as well as S-C and S-Z fabrics defined by orientated mica. The mineralogy of these rocks mainly includes illite, quartz, vermiculite, kaolinite, K-feldspar? and interstratified illite/smectite I/S R1 and I/S R0 (Fig. 7B).

The b parameter values ranges from 9.03 Å to 8.98 Å showing a decreasing pattern from southwest to northeast (Fig. 8), indicating that the analyzed samples present medium-to low-pressure baric types and associated medium (25–35 °C/km) to high thermal gradients (> 35 °C/km), respectively (Guidotti and Sassi, 1986). The KI_{ClIS} values are comparable for all analyzed samples spanning between 0.42 and 0.67 $\Delta^{\circ}2\theta$, belonging to the lower anchizone and the diagenetic zone (Warr and Ferreiro Mählmann, 2015), with a fairly defined trend increasing towards the northeast (Fig. 8).

4.5. Zircon U-Pb geochronology

One sample from a 20 cm-thick non-deformed dyke intruding deformed mudstones and sandstones from the upper member of the Abejorral Formation was collected for geochronological analyses. This rock shows a porphyritic texture defined by amphibole and plagioclase phenocrysts suggesting an intermediate andesitic composition. Forty-one zircons were analyzed, showing euhedral prismatic forms with minor broken edges. Cathodoluminescence images show oscillatory zonation with Th/U ratios between 0.2 and 0.7, typical of magmatic zircons (Rubatto, 2002; Vavra et al., 1999). The sample yielded a

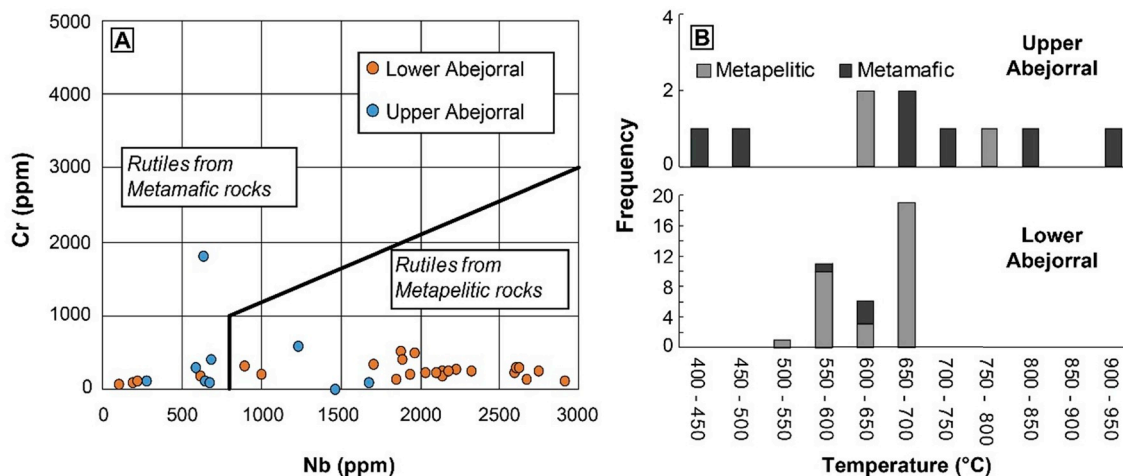


Fig. 6. A) Nb vs. Cr classification diagram of rutile after Meinhold et al. (2008); B) Histogram showing the estimated temperatures calculated from the Zr-in-rutile thermometer of Watson et al. (2006).

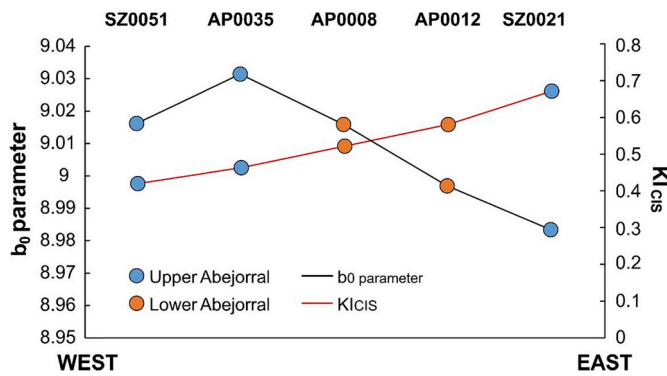


Fig. 8. b_0 parameter and K_{ICIS} values for analyzed samples, showing the transition from low-grade metamorphic (anchizone) values to diagenetic values from southwest to northeast.

weighted mean average age of 60.4 ± 0.4 Ma, which is interpreted as the crystallization age of the dyke (Fig. 9).

5. Discussion

5.1. Sedimentary provenance: implications on the erosional patterns of the Central Cordillera basement

The sandstones of both the lower and the upper members of the Abejorral Formation were mainly sourced from the pre-Cretaceous basement of the Central Cordillera as suggested by the petrographic and U-Pb detrital geochronological analyses presented in Zapata et al. (2019) (see a summary of geochronological constraints in Table 2). However, our new varietal analyses of metamorphic lithic fragments and hornblende grains, together with the results of the geochemical analysis of detrital rutile grains, allowed us to propose westerly metabasic rocks of the Arquía Complex as a potential source as well, likewise the observations of Avellaneda-Jiménez et al. (2019) in coeval units cropping out farther to the south.

The most striking aspect of the petrographic analysis conducted by Zapata et al. (2019) is the appearance of volcanic lithic fragments in the upper member of the Abejorral Formation, which according to our new data, are mostly felsitic and colorless to green-brown vitreous, suggesting intermediate-acid compositions (Dickinson, 1970; Schmincke, 1982). These observations are concordant with the andesitic character of the syn-sedimentary extensional magmatism and the associated Early

Cretaceous (~103–120 Ma) detrital zircon ages documented by Zapata et al. (2019) in sandstones from the upper member (Table 2). The previously published data, and our new results, show that the volcanic lithics are still less abundant than the sedimentary and metamorphic fragments, which is in agreement with a spatially limited dispersion of juvenile material in a deepening marine basin more likely associated with effusive rather than explosive volcanism. The increase in the sedimentary and metamorphic lithic fragments in sandstones and conglomerates of the upper member of the Abejorral Formation, as well as the appearance of plutonic clasts in minor proportion, reveal the ongoing unroofing of the source areas as well as reworking of formerly accumulated sediments (i.e. lower member) indicating tectonic instability in the basin.

The metamorphic lithic fragments also revealed an interesting feature indicating the appearance of metapsammitic and metafelsitic sources in the upper member of the Abejorral Formation, although no important variations were observed regarding the metamorphic grade of source rocks. The heavy mineral assemblages indicate the dominance of stable and ultrastable species such as clinozoisite-zoisite, muscovite, staurolite, zircon, rutile and tourmaline, which are minerals commonly found in the middle-lower crust associated with low-medium-grade metapelitic rocks (Garzanti and Andò, 2007), and have been widely reported in both the Cajamarca and Arquía Complexes (Table 1).

The HCI values obtained during our heavy mineral analysis, suggest that both the lower and the upper members of the Abejorral Formation were mainly sourced from metapelitic and/or metabasic terranes in lower amphibolite up to granulite facies, as indicated by the high content of brown hornblende (Andò et al., 2013). Blue-green hornblende, the less abundant variety in the analyzed samples, is commonly related to dissected arc-batholiths (Garzanti and Andò, 2007). This, together with the scarce Jurassic detrital U-Pb ages (Table 2) suggest that ca. 150–200 Ma intrusive units of the Central Cordillera were limited sources for the Abejorral Formation and coeval units. Likewise, the Lower Cretaceous volcanic rocks of the Central Cordillera are mostly composed of plagioclase and clinopyroxene, which are occasionally altered to fibrous pale green amphibole (Rodríguez and Celada-Arango, 2018). Therefore, most hornblende grains were likely derived from the metamorphic terranes (Cajamarca and Arquía Complexes) and are useful as proxies to document the progressive unroofing of deeper crustal levels and or/the incorporation of more distal higher-grade units. Thus, despite the similarities in the heavy minerals assemblage of both members of the Abejorral Formation, the relative increase in the abundance of green-brown and brown hornblende upward in the

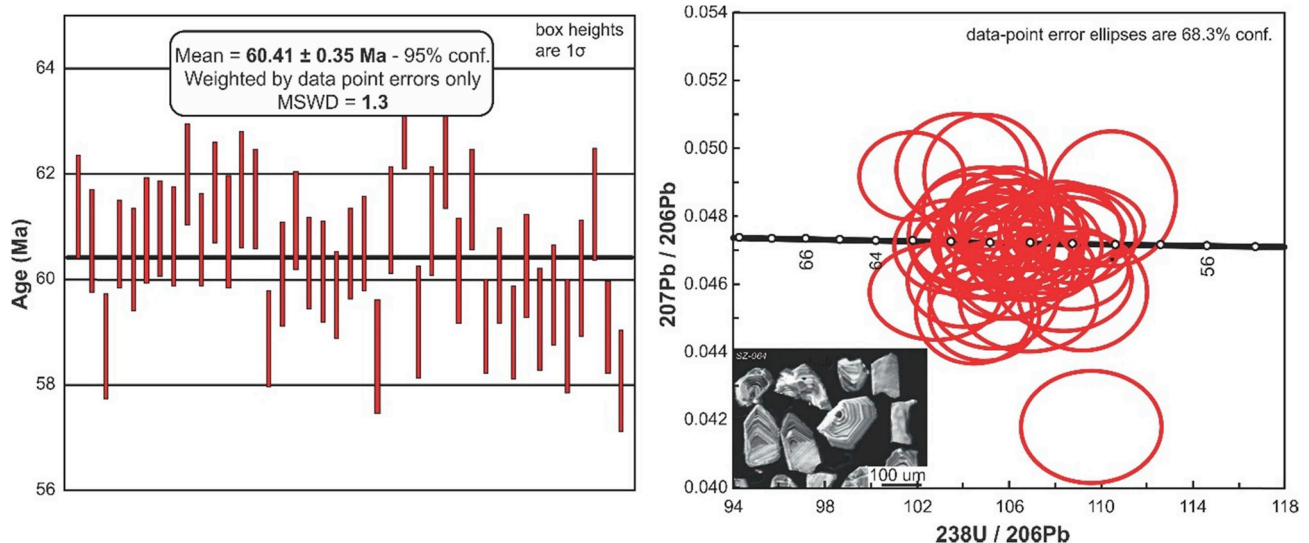


Fig. 9. Weighted average age and Tera-Wasserburg diagram for the analyzed sample (SZ-064).

Table 2

Summary of the available geochronological constraints for volcano-sedimentary rocks of the Abejorral Formation and the Quebradagrande Complex.

Geological Unit	Analyzed Rock	Crystallization Age	Reported Max. Accumulation Age	Detrital Age Peaks (<i>Inherited Ages</i>)
lower member - Abejorral Formation ^a	Sandstone	NA	149.5 ± 2.7 Ma 236.1 ± 3.5 Ma	~ 153–180 Ma, ~ 240–278 Ma, ~ 530–650 Ma, > 1000 Ma
upper member - Abejorral Formation ^a	Sandstone	NA	125.3 ± 2.3 Ma 104.3 ± 2.2 Ma 103.9 ± 2.8 Ma	~ 100–150 Ma, ~ 240–270 Ma, ~ 450–600 Ma, > 1000 Ma
Quebradagrande Complex ^b	Andesite	103.1 ± 1.5 Ma	NA	(~ 220–240 Ma, ~ 400 Ma)
	Andesitic Tuff	111.5 ± 7.9 Ma	NA	(~ 340–2200 Ma)
	Porphyry	103.5 ± 1.8 Ma	NA	NA
	Sandstone	NA	149.2 ± 6.1 Ma	~ 500–600 Ma, > 900 Ma
	Sandstone	NA	84.0 ± 0.5 Ma	~ 80–85 Ma, ~ 230–270 Ma, ~ 400–600 Ma, > 900 Ma
	Sandstone	NA	336 Ma	~ 300–400 Ma, ~ 500–700 Ma, > 1000 Ma
	Andesite	83.2 ± 0.7 Ma	NA	(~ 113 Ma, > 1000 Ma)
Metatuff	114.3 ± 3.8 Ma	NA	(~ 140 Ma)	
	Diorite	112.9 ± 0.8 Ma	NA	NA

^a Zapata et al. (2019).^b Avellaneda-Jiménez et al. (2019); Cochran et al. (2014b); Villagómez et al. (2011); Zapata et al. (2019).

sequence may indicate the progressive unroofing of deeper crustal levels and/or incorporation of new exposed higher-grade source areas as expected for tectonically active ranges (e.g. Uddin and Lundberg, 1998).

The appearance of very low-to very high-grade metapsammitic/metafelsitic lithic fragments in the upper member of the Abejorral Formation (apparently absent in the lower member), may suggest the progressive inclusion of deeper gneissic rocks by unroofing of the schists cover of the Central Cordillera pre-Cretaceous basement. Our results of rutile mineral chemistry suggest that medium-grade metapelitic rocks mainly sourced the lower member of the Abejorral Formation, whereas the upper member contains rutile grains mostly derived from medium-to high-grade metamafic units, as well as from low-grade rocks which seems to be absent in the provenance record of the lower member. As mentioned above, the HCI indexes also slightly increase towards the upper Abejorral Formation (up to 83.3) indicating the appearance of high-grade metagabbroic sources (Andò et al., 2013).

A plausible erosional pattern suggested from our provenance analysis, when integrated with previously published data, may result from (1) both the progressive exhumation of deeper crustal levels and the lateral migration of the erosional front and/or (2) the incorporation of more distal sources, as expected for a growing extensional basin (e.g. Schneider et al., 2017). The upward increase in the HCI values, together with the appearance of higher-grade metapelitic and metafelsitic grains, may be the consequence of the unroofing of the pre-Cretaceous rocks of the Cajamarca Complex, which is dominantly composed of quartz- and feldspar-rich schists and gneisses (Table 1). Furthermore, the compositional change from metapelitic towards dominantly metabasic units of low-to high-grade metamorphism, may be explained by the incorporation of westerly units of the Arquía Complex, which include rocks of greenschist to blueschist and retrograde eclogites facies with common basaltic-gabbroic protoliths (Avellaneda-Jiménez et al., 2019 and references therein).

The analysis of P-T trajectories in the Oligocene-Miocene back-arc regions of the Aegean and Tyrrhenian regions has shown that ongoing extension led to the inclusion of subduction-complex-related metamorphic rocks in the back-arc basin erosional fronts, serving as a first-order mechanism responsible for the exhumation of such terranes (Jolivet et al., 1994). This scenario may explain the erosional pattern indicated by our provenance analysis, which suggests that during the transition from the lower to the upper members of the Abejorral Formation, the source areas incorporated both deeper medium-to high-grade crustal levels, as well as more distal low-to high-grade units (Fig. 10). This, together with the switching from the dominance of pelitic protoliths to higher-grade metamafic source rocks evidenced in the rutile mineral chemistry and the HCI values, allow us to infer that

during the accumulation of the upper Abejorral Formation, the subduction-related Arquía Complex could have played an important role as sediment source (Fig. 10). Recently published provenance constraints have also documented the partial exhumation and erosion of the Arquía Complex during the Early Cretaceous, as suggested by the presence of glaucophane, olivine, spinel, together with high-pressure detrital garnets in Early Cretaceous (Aptian-Albian) sediments from the Quebradagrande Complex (Avellaneda-Jiménez et al., 2019). This suggests that our observations are comparable with coeval units exposed farther to the south.

5.2. Geodynamic setting during basin opening and deformation

Although we are aware that our database is limited, mainly due to the absence of continuous exposures of the sedimentary sequences studied in this work, some important considerations on the tectonic setting on which the Abejorral Formation was accumulated and subsequently deformed, are allowed from our crystallochemical indexes constraints. As discussed above, the *b* parameter values show a well-defined decreasing pattern towards the northeast as one gets farther from the RFS, with the K_{ClS} values increasing in the same direction. Samples located in the northeastern part of the study area (AP-012-lower and SZ-021-upper member) seem to preserve a primary clastic fabric and belong to the diagenetic zone, whereas rocks characterized by a more developed low-grade metamorphic structure are preferentially located towards the southwest (AP-008-lower, AP-035- and SZ-051-upper member) and belong to the lower anchizone. It is noticeable that the deformational/diagenetic fabrics and the thermobarometric constraints are not a function of the stratigraphic position of the analyzed samples. Those constraints may result from their location respect to major fault systems and therefore the locus of higher stress, such as the RFS. We interpret that the white mica *b* parameter data obtained from primary sedimentary samples, reflect the tectonic setting where the Abejorral Formation was accumulated, which according to the measured crystallochemical indexes, would have been characterized by a high heat-flow regime with thermal gradients above 25–35 °C/km (Guidotti and Sassi, 1986). Conversely, the thermobarometric constraints obtained from samples located towards the southwest, nearby the influence of the RFS, rather likely reflect the post-depositional deformational history of the Abejorral Formation and coeval units located in a similar structural position (e.g. Quebradagrande Complex).

Our thermobarometric constraints provided independent evidence that points for high-heat flow during the accumulation of both the lower and upper Abejorral Formation (high K_{ClS} and low *b* parameter values). This, together with the transgressive character of this unit

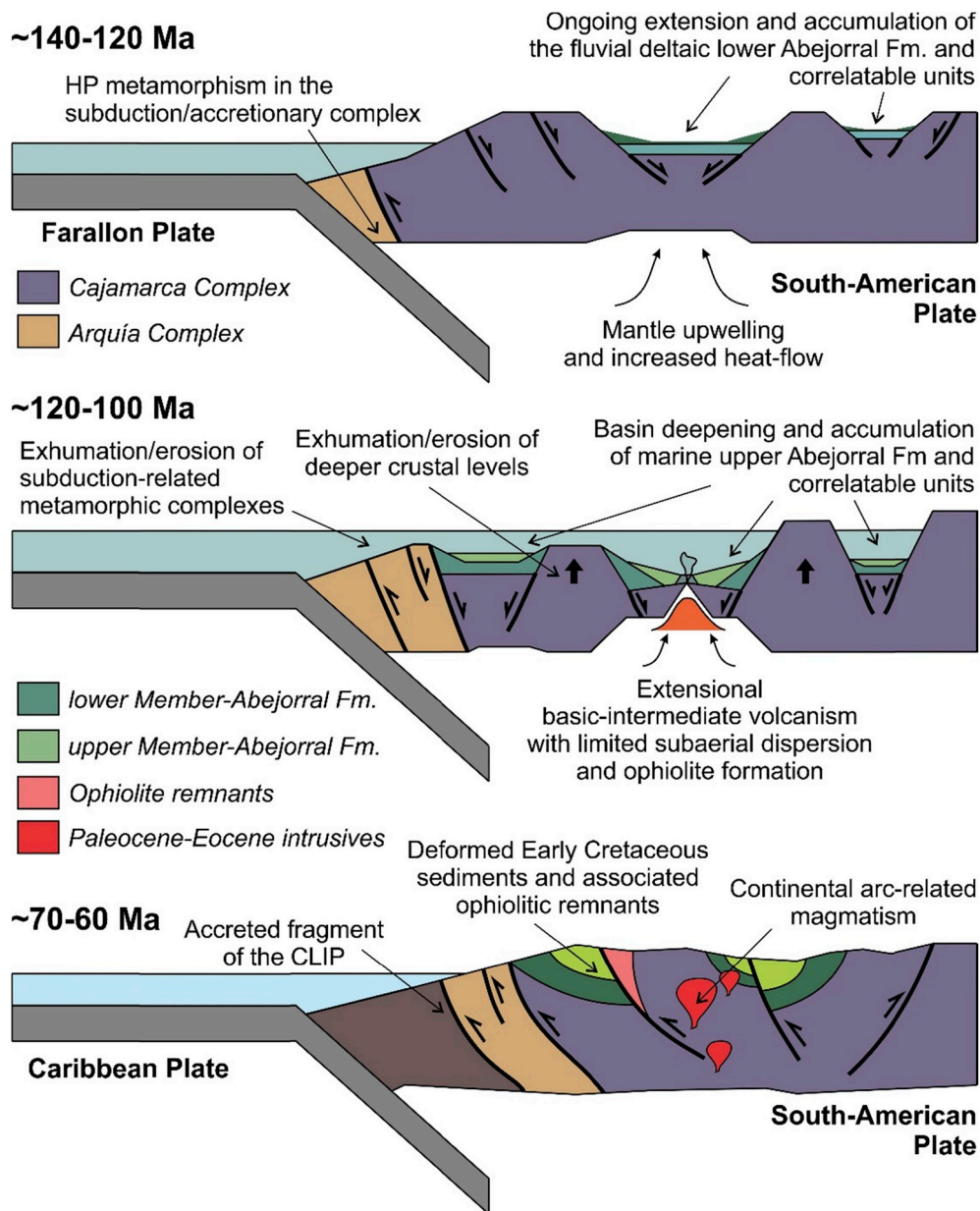


Fig. 10. Schematic diagram showing the regional geodynamic setting for the accumulation and subsequent deformation of rocks from the Abejorral Formation in the tectonic framework of a growing back-arc basin.

marked by the transition from fluvial-deltaic towards fully marine environments, as well as the occurrence of coeval intermediate-basic magmatism and ophiolite remnants, are used here to buttress the back-arc setting for the accumulation of the Early Cretaceous units discussed in this work. The presence of Permian-Triassic continental rocks both underlying and flanking these sequences also supports this scenario on which extensional tectonics resulted in the formation of marginal basins and subsequent generation of oceanic crust. The progressive crustal unroofing, as well as the incorporation of more distal subduction-related metamorphic rocks, would have resulted either from widening the erosional front or the reactivation of fault structures facilitating the exhumation of western domains (Fig. 10).

The results of this contribution also favor the back-arc hypothesis for the tectonic setting on which the Early Cretaceous volcano-sedimentary rocks of the Central Cordillera were accumulated (Zapata et al., 2019). As mentioned above, some authors have interpreted this stratigraphic record as associated with a foreland basin (e.g. Spikings et al., 2015). These authors based their interpretation on the apparent

absence of magmatism younger than ~ 114 Ma, and an accelerated period of exhumation between ~ 120 and 100 Ma, which is attributed to the transition from extensional to compressional tectonics. Furthermore, by assuming an allochthonous or parautochthonous origin of Early Cretaceous volcanic rocks exposed in the Central Cordillera, an alternative passive margin setting has been proposed for the accumulation of coeval siliciclastic rocks (i.e. Abejorral Formation; Pardo-Trujillo et al., 2002; Rodríguez and Celada-Arango, 2018). However, the recently published geochronological constraints by Zapata et al. (2019) showed that magmatism in the Central Cordillera was rather continuous at least until ca. 100 Ma (Table 2). Additionally, Duque-Trujillo et al. (2019) have published a review on the available geochronological data for plutonic rocks spatially associated with the here discussed Early Cretaceous volcano-sedimentary sequences, and suggested that these units record protracted magmatism between ~ 97 and ~ 60 Ma along the cordillera. Therefore, the cooling/exhumation ca. 120 - 100 Ma of basement rocks of the proto-Central Cordillera (Spikings et al., 2015; Villagómez and Spikings, 2013) was likely triggered by

extensional tectonics on a deepening back-arc system (Zapata et al., 2019, this work) growing at an active continental margin.

Sandstone samples located to the southwest show low-grade metamorphic fabrics, which rather document the P-T conditions on which the Abejorral Formation was subsequently deformed after its deposition. The b parameter and K_{CIS} values of these rocks suggest low-medium pressure facies and thermal gradients between 25 °C and 35 °C/km (Guidotti and Sassi, 1986). As mentioned above, these are close to the RFS, where both Cretaceous volcano-sedimentary rocks of the Quebradagrande Complex and the Abejorral Formation are tectonically juxtaposed with the Arquía Complex (Avellaneda-Jiménez et al., 2019; González, 2001; Vinasco and Cordani, 2012; Zapata et al., 2019). The RFS has been interpreted as the suture zone between the continental paleomargin and accreted exotic oceanic terranes derived from the Caribbean plate since the Late Cretaceous-Paleocene (Restrepo and Toussaint, 1988; Villagómez and Spikings, 2013). Nevertheless, this major fault system has been tectonically reactivated through the Cenozoic (Suter et al., 2008; Vinasco and Cordani, 2012), as the consequence of over-imposed collisional and subduction-related tectonics (León et al., 2018).

The ca. 60 Ma crystallization age yielded by the non-deformed porphyry cutting the deformational fabric of rocks from upper member of the Abejorral Formation suggests that this sequence experienced a deformational episode prior to the middle Paleocene. Further geochronological and more extensive chemical/mineralogical analyses of mineral phases associated with the deformational fabrics identified in rocks from the Abejorral Formation will allow directly discriminating the timing and nature of the responsible tectonic mechanisms for such deformation. However, by considering the proposed tectonic scenario for the Cretaceous-Paleocene, we speculate that the deformational event affecting the upper member would have been triggered either by a transition from extensional to compressional tectonics at ca. 100 Ma (Zapata et al., 2019), or by the collision of the Caribbean Large Igneous Province (CLIP) at ca. 70-60 Ma (Villagómez and Spikings, 2013). The compressional event, likely triggered by regional-scale plate kinematics (Zapata et al., 2019), caused the closure of the back-arc basin on which the Lower Cretaceous rocks discussed in this work accumulated. The Campanian-Paleocene collisional episode has been well-documented and is linked with the onset of the Andean orogeny and the evolution of a Paleocene-Eocene continental arc in the Central Cordillera (Bayona, 2018; Bustamante et al., 2017b; Cardona et al., 2018).

The ca. 90-80 Ma arc-related volcanic, plutonic and sedimentary rocks of the Quebradagrande Complex both intrude and unconformably overly the Abejorral Formation. This unit has been interpreted as the record of the transition from extensional to compressional tectonics in northwestern Colombia (Zapata et al., 2019). A recent structural analysis on rocks from the Quebradagrande Complex suggests that this unit presents a west-vergent well-defined ductile deformational fabric with inverse-dextral kinematic features resulting from strain partitioning under transpressional tectonics (Moreno-Sánchez et al., 2016). The Abejorral Formation and coeval units further to the south show similar deformational structures such as northeast-dipping thrust faults and west-vergent asymmetric folds together with mylonitic fabrics (Avellaneda-Jiménez et al., 2019; González, 2001; Zapata et al., 2019), which may also be associated with a transpressional tectonic regime. The strong structural and geometrical similarities between the deformational features of rocks from the Lower Cretaceous units and the Upper Cretaceous Quebradagrande Complex allow speculating that the observed structural imprint may result from a shared tectonic history, including the Late Cretaceous-Paleocene collisional episode and the Cenozoic collision/subduction regimes.

6. Conclusions

The integrated provenance analysis of sandstones from the Abejorral Formation allowed us to identify major changes of source

areas composition, which have not been documented so far from conventional sandstone petrography and detrital zircon geochronology. Medium-to high-grade metapelitic and metamafic rocks, similar to those described within the Cajamarca and Arquía Complexes, likely sourced the Abejorral Formation as previously suggested. Our hornblende varietal study and rutile mineral chemistry data suggest that the upper member of the Abejorral Formation includes material dominantly derived from both higher-grade rocks and low-grade metamafic units, as well as volcanic lithic fragments of intermediate composition that were absent in the lower member. Thermobarometric constraints from the clay mineralogy allowed us to document the presence of two groups of samples with contrasting fabrics. A first set of samples preserving primary diagenetic features suggests a high-heat flow (> 25–35 °C/km) during their accumulation. Conversely, the second set of samples shows low-grade metamorphic fabrics together with a thermobarometric signature belonging to the anchizone, rather reflecting low-to medium-pressure and medium thermal gradients deformational conditions.

Our results enable us to buttress the previously proposed back-arc setting for the accumulation of the Abejorral Formation. The back-arc scenario was marked by the progressive unroofing of the basement rocks of the Central Cordillera as well as the changes of the extensional front during basin opening that resulted in the incorporation of deeper and/or more distal source areas, including the Cajamarca Complex (to the east) and the subduction-related Arquía Complex (to the west). Both the lower and upper members of the Abejorral Formation and coeval units likely record a complex deformational history caused by over-imposed events and tectonic regimes. Geochronological and field observations suggest that these rocks include a deformational episode prior to ca. 60 Ma, triggered either by a switching from extension to compression in the middle Cretaceous linked to regional-scale plate kinematics or by the Late Cretaceous-Paleocene collision of the CLIP with northwestern South America.

Acknowledgements

This research was funded by the National University of Colombia (Hermes) through projects 25452, 25340, 29182, 18593 and 24208, the Fundación para la Promoción de la Investigación y la Tecnología (FPIT, project 3.451), and the Fondo para la Investigación Científica y Técnica of Argentine (FONCYT PICT 2015–1092 and FONCYT PICT 2017–3177). We are thankful to A. Patiño for her help during acquisition of mineral chemistry data. Members of the EGO Research Group who participated during the 2014 fieldwork campaigns and discussions are deeply acknowledged. The quality of this manuscript was certainly improved by the revisions of German Bayona and Cristian Vallejo, as well as by the editorial care of Andrés Folguera.

Appendix A. Supplementary data

Supplementary data to this article can be found online at <https://doi.org/10.1016/j.jsames.2019.102229>.

References

- Álvarez, J., 1987. Geología del Complejo Ofiolítico de Pácora y secuencias relacionadas de arco de isla (Complejo Quebradagrande).
- Andò, S., Morton, A., Garzanti, E., 2013. Metamorphic grade of source rocks revealed by chemical fingerprints of detrital amphibole and garnet. *Geol. Soc. London, Spec. Publ.* 386. <https://doi.org/10.1144/SP386.5>.
- Arévalo, O.J., Mojica, J., Patarroyo, P., 2001. Sedimentitas del Aptiano tardío al sur de Pijao, Quebrada La Maizena, flanco Occidental de la Cordillera Central, Departamento de Quindío, Colombia. *Geol. Colomb.* 26, 29–43.
- Atherton, M.P., Webb, S., 1989. Volcanic facies, structure, and geochemistry of the marginal basin rocks of central Peru. *J. South Am. Earth Sci.* 2, 241–261. [https://doi.org/10.1016/0895-9811\(89\)90032-1](https://doi.org/10.1016/0895-9811(89)90032-1).
- Avellaneda-Jiménez, D.S., Cardona, A., Valencia, V., Barbosa, J.S., Jaramillo, J.S., Monsalve, G., Ramírez-Hoyos, L.F., 2019. Erosion and regional exhumation of an Early Cretaceous subduction/accretion complex in the Colombian Andes. *Int. Geol. Rev.* <https://doi.org/10.1080/00206814.2019.1596042>.

- Bayona, G., 2018. El inicio de la emergencia de los Andes del norte: una perspectiva a partir del registro tectónico-sedimentológico del Coniaciano al Paleoceno. *Rev. la Acad. Colomb. Ciencias Exactas, Físicas y Nat.* 42, 1–15. <https://doi.org/10.18257/racefyn.632>.
- Blanco-Quintero, I.F., García-Casco, A., Toro, L.M., Moreno, M., Ruiz, E.C., Vinasco, C.J., Cardona, A., Lázaro, C., Morata, D., 2014. Late Jurassic terrane collision in the northwestern margin of Gondwana (Cajamarca complex, eastern flank of the central cordillera, Colombia). *Int. Geol. Rev.* 56, 1852–1872. <https://doi.org/10.1080/00206814.2014.963710>.
- Botero, G., 1963. Contribución al conocimiento de la geología de la zona central de Antioquia. *An. la Fac. Minas* 57, 3–101.
- Braz, C., Seton, M., Flament, N., Müller, R.D., 2018. Geodynamic reconstruction of an accreted Cretaceous back-arc basin in the Northern Andes. *J. Geodyn.* 121, 115–132. <https://doi.org/10.1016/j.jog.2018.09.008>.
- Burov, E., Poliakov, A., 2003. Erosional forcing of basin dynamics: new aspects of syn- and post-rift evolution. *Geol. Soc. London, Spec. Publ.* 212, 209–223.
- Bustamante, A., 2008. Geobarometría, geoquímica, geocronología e evolución tectónica das rochas de fácies xisto azul nad áreas de Jambaló (Cauca) e Barragán (Valle del Cauca), Colombia. Universidade de São Paulo.
- Bustamante, A., Juliani, C., 2011. Unraveling and antique subduction process from metamorphic basement around Medellín city, Central Cordillera of Colombian Andes. *J. South Am. Earth Sci.* 32, 210–221. <https://doi.org/10.1016/j.jsames.2011.06.005>.
- Bustamante, A., Juliani, C., Hall, C.M., Essene, E.J., 2011. 40Ar/39Ar ages from blueschists of the Jambaló region, Central Cordillera of Colombia: implications on the styles of accretion in the Northern Andes. *Geol. Acta* 9, 351–362. <https://doi.org/10.1344/105.000001697>.
- Bustamante, A., Vidal, L., Franco, J.P., Pulido, D., Ochoa, V., 2013. Esquistos de moscovita-cloritoide en la región de El Retiro, Antioquia: geotermometría y significado tectónico. *Boletín Ciencias La Tierra* 33, 5–16.
- Bustamante, C., Archanjo, C.J., Cardona, A., Bustamante, A., Valencia, V.A., 2017a. U-Pb ages and Hf isotopes in zircons from parautochthonous Mesozoic terranes in the western margin of Pangea: implications for the terrane configurations in the northern Andes. *J. Geol.* 125, 487–500.
- Bustamante, C., Archanjo, C.J., Cardona, A., Vervoort, J.D., 2016. Late Jurassic to Early Cretaceous plutonism in the Colombian Andes: a record of long-term arc maturity. *Geol. Soc. Am. Bull.* 128, 1762–1779. <https://doi.org/10.1130/B31307.1>.
- Bustamante, C., Cardona, A., Archanjo, C.J., Bayona, G., Lara, M., Valencia, V., 2017b. Geochemistry and isotopic signatures of Bayona plutonic and detrital rocks of the Northern Andes of Colombia: a record of post-collisional arc magmatism. *Lithos* 277, 199–209. <https://doi.org/10.1016/j.lithos.2016.11.025>.
- Cardona, A., León, S., Jaramillo, J.S., Montes, C., Valencia, V., Vanegas, J., Bustamante, C., Echeverri, S., 2018. The Paleogene arcs of the northern Andes of Colombia and Panama: insights on plate kinematic implications from new and existing geochemical, geochronological and isotopic data. *Tectonophysics* 749, 88–103. <https://doi.org/10.1016/j.tecto.2018.10.032>.
- Cardona, A., Valencia, V., Garzón, A., Montes, C., Ojeda, G., Ruiz, J., Weber, M., 2010. Permian to Triassic I to S-type magmatic switch in the northeast Sierra Nevada de Santa Marta and adjacent regions, Colombian Caribbean: tectonic setting and implications within Pangea paleogeography. *J. South Am. Earth Sci.* 29, 772–783. <https://doi.org/10.1016/j.jsames.2009.12.005>.
- Chang, Z., Vervoort, J.D., McClelland, W.C., Knaack, C., 2006. U-Pb dating of zircon by LA-ICP-MS. *Geochim. Geophys. Geosyst.* 7, 1–14. <https://doi.org/10.1029/2005GC001100>.
- Cochrane, R., Spikings, R.A., Gerdas, A., Ulianov, A., Mora, A., Villagómez, D., Putlitz, B., Chiaradia, M., 2014a. Permo-Triassic anatexis, continental rifting and the disassembly of western Pangaea. *Lithos* 190–191, 383–402. <https://doi.org/10.1016/j.lithos.2013.12.020>.
- Cochrane, R., Spikings, R.A., Gerdas, A., Winkler, W., Ulianov, A., Mora, A., Chiaradia, M., 2014b. Distinguishing between in-situ and accretionary growth of continents along active margins. *Lithos* 202–203, 382–394. <https://doi.org/10.1016/j.lithos.2014.05.031>.
- Cochrane, R.S.J., 2013. U-pb Thermochronology, Geochronology and Geochemistry of NW South America: Rift to Drift Transition, Active Margin Dynamics and Implications for the Volume Balance of Continents. Université de Genève.
- Corrado, S., Aldega, L., Perri, F., Critelli, S., Muto, F., Schito, A., Tripodi, V., 2018. Detecting Syn-Orogenic Extension and Sediment Provenance of the Cliento Wedge Top Basin (Southern Apennines, Italy): Mineralogy and Geochemistry of Fine-Grained Sediments and Petrography of Dispersed Organic Matter. *Tectonophysics* In Press <https://doi.org/10.1016/j.tecto.2018.10.027>.
- Correa, A.M., 2007. Petrogenesis and Evolution of the Aburra Ophiolite, Colombian Andes, Central Range. Universidade de Brasília.
- Correa, A.M., Martens, U., Restrepo, J.J., Ordoñez-Carmona, O., Pimentel, M.M., 2005. Subdivisión de las metamorfitas básicas de los alrededores de Medellín - cordillera Central de Colombia. *Rev. la Acad. Colomb. Ciencias Exactas, Físicas y Nat.* 29, 325–343.
- Degeling, H.S., 2003. Zr Equilibria in Metamorphic Rocks. Australian National University.
- Dickinson, W.R., 1970. Interpreting detrital modes of graywacke and arkose. *J. Sediment. Petrol.* 40, 695–707.
- Duarte, E., Cardona, A., Lopera, S., Valencia, V., Estupiñán, H., 2018. Provenance and diagenesis from two stratigraphic sections of the lower cretaceous caballos formation in the upper Magdalena Valley: geological and reservoir quality implications. *Ciencia, Tecnol. y Futur.* 8, 5–29. <https://doi.org/10.29047/01225383.88>.
- Duarte, E., Cardona, A., Valencia, V., 2015. Procedencia y relaciones estratigráficas de la Formación Caballos en el Valle Superior del Magdalena: hipótesis preliminares de su relación con el clima y la situación tectónica cambiante del Cretácico Inferior en los Andes del Norte. In: XV Congreso Colombiano de Geología. Bucaramanga, Colombia.
- Duque-Trujillo, J., Bustamante, C., Solari, L., Gómez-Mafla, A., Toro-Villegas, G., Hoyos, S., 2019. Reviewing the Antioquia batholith and satellite bodies: a record of Late Cretaceous to Eocene syn- to post-collisional arc magmatism in the Central Cordillera of Colombia. *Andean Geol.* 46, 82–101. <https://doi.org/10.5027/andgeoV46n1-3120>.
- Ernst, W.G., 1963. Significance of phengitic micas from low-grade schists. *Am. Mineral.* 48, 1357–1373.
- Folk, R.L., 1980. *Petrology of Sedimentary Rocks*. Hemphill Publishing Company, Austin, Texas.
- García-Ramírez, C.A., Ríos-Reyes, C.A., Castellanos-Alarcón, O.M., Mantilla-Figueroa, L.C., 2017. Petrology, geochemistry and geochronology of the Arquía complex's metabasites at the pijao-génova sector, central cordillera, Colombian Andes. *Bol. Geol.* 39.
- Garzanti, E., Andò, S., 2007. Heavy-mineral concentration in modern sands: implications for provenance interpretation. In: In: Mange, M.A., Wright, D.T. (Eds.), *Heavy Minerals in Use*, vol. 58. Elsevier, Amsterdam, pp. 517–545. *Developments in Sedimentology Series*.
- Garzanti, E., Doglioni, C., Vezzoli, G., Andò, S., 2007. Orogenic belts and orogenic sediment provenance. *J. Geol.* 115, 315–334.
- Garzanti, E., Vezzoli, G., 2003. A classification of metamorphic grains in sands based on their composition and grade. *J. Sediment. Res.* 73, 830–837. <https://doi.org/10.1306/012203730830>.
- Gómez-Cruz, A.D.J., 1995. Edad y origen del Complejo Metasedimentario de Aranzazu-Manizales en los alrededores de Manizales (Departamento de Caldas, Colombia). *Geol. Colomb.* 19, 83–93.
- Gómez-Cruz, A.D.J., Moreno-Sánchez, M., Pardo-Trujillo, A., 1995. Edad y Origen del Complejo metasedimentario Aranzazu-Manizales en los Alrededores de Manizales (Departamento de Caldas, Colombia). *Geol. Colomb.* 19, 83–93.
- Gómez-Tapias, J., Montes-Ramírez, N.E., Almanza-Meléndez, M.F., Alcárcel-Gutiérrez, F.A., Madrid-Montoya, C.A., Diederix, H., 2017. Geological map of Colombia. *Episodes* 40, 201–212. <https://doi.org/10.18814/epiugs/2017/v40i3/017023>.
- González, H., 2001. Mapa Geológico del Departamento de Antioquia. Memoria Explicativa Escala 1:400.000.
- González, H., 1997. Metagabros y eclogitas asociadas en el área de Barragán, Departamento del Valle, Colombia. *Geol. Colomb.* 22, 151–170.
- González, H., 1980. Geología de las Planchas 167 (Sonsón) y 187 (Salamina). *Bol. Geol. - Ingeominas* 23, 1–174.
- Guidotti, C.V., Sassi, F.P., 1986. Classification and correlation of metamorphic facies series by means of muscovite b data from low-grade metapelites. *Neues Jahrbuch Mineral. Abhand.* 153, 363–380.
- Guidotti, C.V., Sassi, F.P., Blencoe, J.G., 1989. Compositional controls on the a and b cell dimensions of 2M1 muscovite. *Eur. J. Mineral.* 1, 71–84.
- Jolivet, L., Daniel, J.M., Truffert, C., Goffé, B., 1994. Exhumation of deep crustal metamorphic rocks and crustal extension in arc and back-arc regions. *Lithos* 33, 3–30. [https://doi.org/10.1016/0024-4937\(94\)90051-5](https://doi.org/10.1016/0024-4937(94)90051-5).
- Kisch, H.J., 1991a. Development of slaty cleavage and degree of very-low-grade metamorphism: a review. *J. Metamorph. Geol.* 9, 735–750.
- Kisch, H.J., 1991b. Illite crystallinity: recommendations on sample preparation, X-ray diffraction settings, and interlaboratory samples. *J. Metamorph. Geol.* 9, 665–670.
- Kisch, H.J., Sassi, R., Sassi, F.P., 2006. The b0 lattice parameter and chemistry of phengites from HP/LT metapelites. *Eur. J. Mineral.* 18, 207–222. <https://doi.org/10.1127/0935-1221/2006/0018-0207>.
- Kleppe, K., Betka, P., Clarke, G., Fanning, M., Hervé, F., Rojas, L., Mpodozis, C., Thomson, S., 2010. Continental underthrusting and obduction during the cretaceous closure of the rocas verdes rift basin, cordillera Darwin, patagonian Andes. *Tectonics* 29, n/a-n/a. doi:10.1029/2009TC002610.
- Kübler, B., 1968. Evaluation quantitative du métamorphisme par la cristallinité de l'illite. *Cent. Rech. Pau, Soc. Natl. des Pétales d'Aquitaine, Bull.* 2, 385–397.
- León, S., Cardona, A., Parra, M., Sobel, E.R., Jaramillo, J.S., Glodny, J., Valencia, V., Chew, D., Montes, C., Posada, G., Monsalve, G., Pardo-Trujillo, A., 2018. Transition from collisional to subduction-related regimes: an example from Neogene Panama-Nazca-South-America interactions. *Tectonics* 37, 119–139. <https://doi.org/10.1002/2017TC004785>.
- Ludwig, K.R., 2012. *Isoplot 3.75, A Geochronological Toolkit for Excel*. 5, vol. 75. Berkeley Geochronol. Cent. Spec. Publ.
- Mange, M.A., Maurer, H.F.W., 1992. *Heavy Minerals in Color*. Chapman & Hall, London.
- Marsaglia, K.M., 1992. Petrography and provenance of volcanoclastic sands recovered from the Izu-Bonin arc, leg 126. In: In: Taylor, B., Fujioka, K., Janecek, T.R., Langmuir, C. (Eds.), *Proceedings of the Ocean Drilling Program, Scientific Results*, vol. 126. pp. 139–154.
- Martens, U., Restrepo, J.J., Ordoñez-Carmona, O., Correa-Martínez, A.M., 2014. The tahamí and Anacona terranes of the Colombian Andes: missing links between the south American and Mexican gondwana margins. *J. Geol.* 122, 507–530.
- Martens, U., Restrepo, J.J., Solari, L.A., 2012. Sinifaná metasedimentites and relations with Cajamarca paragneisses of the central cordillera of Colombia. *Boletín Ciencias la Tierra* 32, 99–109.
- Maya, M., González, H., 1995. Unidades litodémicas de la Cordillera Central de Colombia. *Bol. Geol. - Ingeominas* 35.
- McCourt, W.J., Aspdén, J.A., Brook, M., 1984. New geological and geochronological data from the Colombian Andes: continental growth by multiple accretion. *J. Geol. Soc. London* 141. <https://doi.org/10.1144/gsjgs.141.5.0831>.
- Meinhold, G., 2010. Rutile and its applications in earth sciences. *Earth Sci. Rev.* 102, 1–28. <https://doi.org/10.1016/j.earscirev.2010.06.001>.
- Meinhold, G., Anders, B., Kostopoulos, D., Reschmann, T., 2008. Rutile chemistry and thermometry as provenance indicator: an example from Chios Island, Greece. *Sediment. Geol.* 203, 98–111. <https://doi.org/10.1016/j.sedgeo.2007.11.004>.

- Moore, D.M., Reynolds, R.C., 1997. X-Ray Diffraction and Identification and Analysis of Clay Minerals. Oxford University Press.
- Moreno-Sánchez, M., Hincapié, G., Ossa, C.A., Toro-Toro, L.M., 2016. Caracterización geológico-estructural de algunas zonas de cizalla en el Complejo Quebradagrande en los alrededores de Manizales y Villamaría. *Bol. Geol.* 38, 15–27. <https://doi.org/10.18273/revbol.v38n4-2016001>.
- Morton, A.C., 1985. Heavy minerals in provenance studies. In: Zuffa, G.G. (Ed.), *Provenance of Arenites*. Springer Netherlands, pp. 249–277.
- Morton, A.C., Hallsworth, C.R., 1999. Processes controlling the composition of heavy mineral assemblages in sandstones. *Sediment. Geol.* 124, 3–29.
- Munteanu, I., Matenco, L., Dinu, C., Cloetingh, S., 2011. Kinematics of back-arc inversion of the western black sea basin. *Tectonics* 30, TC5004. <https://doi.org/10.1029/2011TC002865>.
- Nivia, A., Marriner, G.F., Kerr, A.C., Tarney, J., 2006. The Quebradagrande complex: a lower cretaceous ensialic marginal basin in the central cordillera of the Colombian Andes. *J. South Am. Earth Sci.* 21, 423–436. <https://doi.org/10.1016/j.jsames.2006.07.002>.
- Orrego, A., Cepeda, H., Rodríguez, G., 1980. Esquitos glaucofánicos en el área de Jambaló, Cauca (Colombia). *Geol. Norandina* 1, 5–10.
- Pardo-Trujillo, A., Moreno-Sánchez, M., Gomez-Cruz, A.D.J., 2002. Estratigrafía de algunos depósitos del Cretáceo Superior en las Cordilleras Central y Occidental de Colombia: implicaciones Regionales. *Geo-Eco-Trop* 26, 113.
- Quiroz, L., 2005. Cartografía y análisis estratigráfico de las formaciones Valle Alto y Abejorral en la región de San Félix, departamento de Caldas, Colombia. Universidad Nacional de Colombia.
- Reimann-Zumsprekel, C.R., Bahlburg, H., Carlotto, V., Boekhout, F., Berndt, J., Lopez, S., 2015. Multi-method provenance model for early Paleozoic sedimentary basins of southern Peru and northern Bolivia (13°–18°S). *J. South Am. Earth Sci.* 64, 94–115. <https://doi.org/10.1016/j.jsames.2015.08.013>.
- Restrepo, J.J., 2008. Obducción y metamorfismo de ofiolitas Triásicas en el flanco Occidental del terreno Tahamí, Cordillera Central de Colombia. *Bol. Ciencias la Tierra* 22, 49–100.
- Restrepo, J.J., Toussaint, J.F., 1988. Terranes and continental accretion in the Colombian Andes. *Episodes* 11, 189–193.
- Restrepo, J.J., Toussaint, J.F., González, H., Cordani, U.G., 1991. Precisiones geocronológicas sobre el Occidente Colombiano. In: *Simposio Sobre Magmatismo Andino Y Su Marco Tectónico*, pp. 1–21. Manizales.
- Ríos-Reyes, C., Castellanos-Alarcón, O., Ríos-Escobar, V., Gómez-Maya, C., 2008. Una contribución al estudio de la Evolución tectono-metamórfica de las rocas de alta presión del Complejo Arquía, Cordillera Central, Andes Colombianos. *Geol. Colomb.* 33, 3–22.
- Rodríguez, C., Rojas, R., 1985. Estratigrafía de la serie Infracretácica en los alrededores de San Félix, Cordillera Central de Colombia. In: Etayo, F., Laverde, F. (Eds.), *Proyecto Cretácico, Publicaciones Especiales Ingeominas*, pp. 1–21.
- Rodríguez, G., Arango, M.I., Zapata, G., Bermúdez, J.G., 2017. Petrotectonic characteristics, geochemistry, and U-Pb geochronology of Jurassic plutons in the Upper Magdalena Valley-Colombia: implications on the evolution of magmatic arcs in the NW Andes. *J. South Am. Earth Sci.* 81, 10–30. <https://doi.org/10.1016/j.jsames.2017.10.012>.
- Rodríguez, G., Celada-Arango, C.M., 2018. Basaltos de San Pablo: un bloque de un arco de islas en el norte de la cordillera Central de Colombia. *Caracterización petrográfica y química*. *Bol. Geol.* 40, 69–85. <https://doi.org/10.18273/revbol.v40n2-2018004>.
- Rubatto, D., 2002. Zircon trace element geochemistry: partitioning with garnet and the link between U-Pb ages and metamorphism. *Chem. Geol.* 184, 123–138.
- Ruiz-Jiménez, E.C., 2013. Geoquímica y trayectorias PT de las rocas metamórficas del Complejo Arquía, entre los municipios de Santafé de Antioquia (Antioquia) y el río Arquía (Caldas). Universidad de Caldas.
- Ruiz-Jiménez, E.C., Blanco-Quintero, I.F., Toro-Toro, L.M., Moreno-Sánchez, M., Vinasco, C.J., García-Casco, A., Morata, D., Gómez-Cruz, A.J., 2012. Geoquímica y petrología de las metabasitas del Complejo Arquía (Municipio de Santafé de Antioquia y Río Arquía, Colombia): implicaciones geodinámicas. *Boletín Ciencias la Tierra* 32, 65–80.
- Sarmiento-Rojas, L.F., Van Wess, L.D., Cloetingh, S., 2006. Mesozoic transtensional basin history of the Eastern Cordillera, Colombian Andes: inferences from tectonic models. *J. South Am. Earth Sci.* 21, 383–411. <https://doi.org/10.1016/j.jsames.2006.07.003>.
- Sassi, F.P., Scolari, A., 1974. The b₀ value of the potassic white micas as a barometric indicator in low-grade metamorphism of pelitic schists. *Contrib. Mineral. Petrol.* 45, 143–152.
- Schmincke, H.-U., 1982. Ash from vitric muds in deep sea cores from the Mariana Trough and fore-arc region (south philippine sea) (sites 453, 454, 455, 458, 459, and SP), deep sea drilling project leg 60. In: Lee, M., Powell, R. (Eds.), *Initial Reports of the Deep Sea Drilling Project*, vol. 60. US Government Printing Office, Washington, DC, pp. 473–481.
- Schneider, S., Hornung, J., Hinderer, M., 2017. Evolution of the northern Albertine Rift reflected in the provenance of synrift sediments (Nkondo-Kaiso area, Uganda). *J. Afr. Earth Sci.* 131, 183–197. <https://doi.org/10.1016/j.jafrearsci.2017.04.012>.
- Siivola, J., Schmid, R., 2007. A Systematic Nomenclature for Metamorphic Rocks: 12. List of Mineral Abbreviations. Recommendations by the IUGS Subcommission on the Systematics of Metamorphic Rocks. Recommendations, web version of 01.02.2007.
- Sláma, J., Košler, J., Condon, D.J., Crowley, J.L., Gerdes, A., Hanchar, J.M., Hortswood, M.S.A., Morris, G.A., Nasdala, L., Norberg, N., Schaltegger, U., Schoene, B., Tubrett, M.N., Whitehouse, M.J., 2008. Plešovice zircon—a new natural reference material for U–Pb and Hf isotopic microanalysis. *Chem. Geol.* 249, 1–35.
- Spikings, R.A., Cochran, R., Villagómez, D., Van der Lelij, R., Vallejo, C., Winkler, W., Beate, B., 2015. The geological history of northwestern South America: from pangaea to the early collision of the caribbean large igneous Province (290 – 75Ma). *Gondwana Res.* 27, 95–139. <https://doi.org/10.1016/j.gr.2014.06.004>.
- Stern, C.R., De Wit, M.J., 2003. Rocas Verdes ophiolites, southernmost South America: remnants of progressive stages of development of oceanic-type crust in a continental margin back-arc basin. *Geol. Soc. London, Spec. Publ.* 218, 665–683. <https://doi.org/10.1144/GSL.SP.2003.218.01.32>.
- Stone, P., Merriman, R.J., 2004. Basin thermal history favours an accretionary origin for the Southern Uplands terrane, Scottish Caledonides. *J. Geol. Soc. London* 161, 829–836.
- Suter, F., Sartori, M., Neuwerth, R., Gorin, G., 2008. Structural imprints at the front of the chocó-panamá interder: field data from the north Cauca valley basin, Central Colombia. *Tectonophysics* 460, 134–157.
- Toussaint, J.F., Restrepo, J.J., 1996. Evolución Geológica de Colombia, Cretácico. Univ. Nac. Colomb. Medellín.
- Uddin, A., Lundberg, N., 1998. Unroofing history of the eastern himalaya and the indoburman ranges: heavy-mineral study of cenozoic sediments from the bengal basin, Bangladesh. *J. Sediment. Res.* 68, 465–472.
- Valencia-Morales, Y.T., Toro-Toro, L.M., Ruiz-Jiménez, E.C., Moreno-Sánchez, M., 2013. Pressure-temperature path of the Arquía Group rocks (NW Colombia): a petrographic analysis from mineral assemblages. *Earth Sci. Res. J.* 17, 141–149.
- Valencia, V.A., Ruiz, J., Barra, F., Gehrels, G., Ducea, M.N., Tittle, S.M., Ochoa-Landin, L., 2005. U-Pb single zircon and Re-Os geochronology from La claridad porphyry copper deposit: insights for the duration of magmatism and mineralization in the nacozari district, sonora, Mexico. *Miner. Depos.* 40, 175–191.
- Vavra, G., Schmidt, R., Gebauer, D., 1999. Internal morphology, habit and U-Th-Pb microanalysis of amphibolite-to-granulite facies zircons: geochronology of the Ivrea zone (Southern Alps). *Contrib. Mineral. Petrol.* 134, 380–404.
- Verdecchia, S., Collo, G., Zandomeni, P.S., Wunderlin, C., Fehrmann, M., 2018. Crystallochemical indexes and geothermobarometric calculations as a multiproxy approach to P-T condition of the low-grade metamorphism: the case of the San Luis Formation, Eastern Sierras Pampeanas of Argentina. *Lithos* 324–325, 385–401. <https://doi.org/10.1016/j.lithos.2018.11.021>.
- Villagómez, D., Spikings, R.A., 2013. Thermochronology and tectonics of the central and western cordilleras of Colombia: early cretaceous-tertiary evolution of the northern Andes. *Lithos* 160–161, 228–249. <https://doi.org/10.1016/j.lithos.2012.12.008>.
- Villagómez, D., Spikings, R.A., Magna, T., Kammer, A., Winkler, W., Beltrán, A., 2011. Geochronology, geochemistry and tectonic evolution of the Western and Central cordilleras of Colombia. *Lithos* 125, 875–896. <https://doi.org/10.1016/j.lithos.2011.05.003>.
- Villamil, T., Pindell, J.L., 1999. Mesozoic paleogeographic evolution of northern South America. *Soc. Sediment. Geol.* 58, 283–318.
- Vinasco, C., Cordani, U.G., 2012. Reactivation episodes of the Romeral Fault system in the northwestern part of the central Andes, Colombia, through 39Ar-40Ar and K-Ar results. *Boletín Ciencias la Tierra* 32, 111–124.
- Vinasco, C., Cordani, U.G., González, H., Weber, M., Pelaez, C., 2006. Geochronological, isotopic, and geochemical data from Permo-Triassic granitic gneisses and granitoids of the Colombian Central Andes. *J. South Am. Earth Sci.* 21, 355–371. <https://doi.org/10.1016/j.jsames.2006.07.007>.
- von Eynatten, H., Dunkl, I., 2012. Assessing the sediment factory: the role of single grain analysis. *Earth Sci. Rev.* 115, 97–120. <https://doi.org/10.1016/j.earscirev.2012.08.001>.
- Warr, L.N., Ferreiro Mählmann, R., 2015. Recommendations for kübler index standardization. *Clay Miner.* 50, 283–286. <https://doi.org/10.1180/claymin.2015.050.3.02>.
- Warr, L.N., Rice, A.H.N., 1994. Interlaboratory standardization and calibration of clay mineral crystallinity and crystallite size data. *J. Metamorph. Geol.* 12, 141–152.
- Watson, E.B., Wark, D.A., Thomas, J.B., 2006. Crystallization thermometers for zircon and rutile. *Contrib. Mineral. Petrol.* 151, 413–433. <https://doi.org/10.1007/s00410-006-0068-5>.
- Weber, K., 1981. Kinematic and metamorphic aspects of cleavage formation in very low-grade metamorphic slates. *Tectonophysics* 78, 291–306. [https://doi.org/10.1016/0040-951\(81\)90018-4](https://doi.org/10.1016/0040-951(81)90018-4).
- Weltje, G.J., von Eynatten, H., 2004. Quantitative provenance analysis of sediments: review and outlook. *Sediment. Geol.* 171, 1–11. <https://doi.org/10.1016/j.sedgeo.2004.05.007>.
- Zapata, S., Cardona, A., Jaramillo, C., Valencia, V., Vervoort, J., 2016. U-Pb LA-ICP-MS geochronology and geochemistry of Jurassic volcanic and plutonic rocks from the Putumayo region (southern Colombia): tectonic setting and regional correlations. *Bol. Geol.* 38, 21–38. <https://doi.org/10.18273/revbol.v38n2-2016001>.
- Zapata, S., Cardona, A., Jaramillo, J.S., Patiño, A., Valencia, V., León, S., Mejía, D., Pardo-Trujillo, A., Castañeda, J.P., 2019. Cretaceous extensional and compressional tectonics in the Northwestern Andes, prior to the collision with the Caribbean oceanic plateau. *Gondwana Res.* 66, 207–226. <https://doi.org/10.1016/j.jgr.2018.10.008>.